表5-4　　トランスポーターの*in vivo* probe基質、阻害剤の例

in vivo probe基質

Transporter	Gene	Substrate	コメント
P-gp	*ABCB1*	Digoxin	安全域が狭いため、試験の安全性の担保が必要。 1mgを超えると、消化管でのP-gpの飽和が起こる可能性あり。 製剤が複数種あり、溶解プロファイルによっては、吸収性に影響がある。 経口投与の場合、消化管吸収と腎クリアランスの両方の影響を拾うこととなる。 バイオアベイラビリティが70-80%と、消化管での相互作用の影響が感度よく見にくい。
		Fexofenadine	安全域が比較的広い。 バイオアベイラビリティが33%と、消化管での相互作用の影響は見やすい。 肝排泄過程にOATPs, MRP2, MRP3が関与。腎排泄過程には、OAT3, MATEsが関与。 消化管吸収過程に未同定の取り込みトランスポーターの存在が示唆。
		Dabigatran etexilate	バイオアベイラビリティが6.5%と、消化管での相互作用の影響は見やすい。 プロドラッグ体しかP-gpの基質にならない。 OATPs, OCTs, OATs, MRP2, BCRPの基質にならない。 解析事例が少なく、バイオアベイラビリティが低い原因の多くがP-gpであるかは検証が必要。
BCRP	*ABCG2*	Sulfasalazine	バイオアベイラビリティが約7%と、消化管での相互作用の影響は見やすい。 BCRPの遺伝子多型(421C>A)によるAUC上昇率が報告の中で最も大きい。 経口投与で2g程度投与しないとBCRPの機能変動の影響がみにくい。 消化管吸収過程に未同定の取り込みトランスポーターの存在が示唆。 プロドラッグで、腸内細菌による切断を受け活性体になるため、腸内細菌叢の個人差も動態に影響。
		Rosuvastatin	消化管アベイラビリティが50%と、消化管での相互作用の影響は見やすい。 BCRPの遺伝子多型(421C>A)によるAUC上昇率が報告の中で2番目に大きい。 肝排泄過程にOATPs, NTCPが関与。腎排泄過程には、OAT3が関与。P-gp, MRP2基質。
OATP1B1	*SLCO1B1*	Pitavastatin	吸収が良好。非代謝性でほぼすべて胆汁中排泄。 OATP1B1の遺伝子多型(521T>C)によるAUC上昇率が報告の中で比較的大きい(2.5-3倍程度) BCRP基質だが、BCRPの遺伝子多型(421C>A)によるAUC上昇は観察されていない。 in vitro実験の結果、肝取り込みに主にOATP1B1が寄与することが示唆されている。 P-gp, MRP2, BCRPの基質となる。
		Pravastatin	非代謝性で、30%程度が腎排泄、残りが胆汁中排泄。 消化管アベイラビリティが約35%と、吸収があまり良好でない。 OATP1B1の遺伝子多型(521T>C)によるAUC上昇率が報告の中で比較的大きい(2倍程度) 肝排泄過程にMRP2が関与。腎排泄過程には、OAT3が関与。
		Rosuvastatin	非代謝性で、30%程度が腎排泄、残りが胆汁中排泄。 消化管アベイラビリティが50%程度。 OATP1B1の遺伝子多型(521T>C)によるAUC上昇率が報告の中で比較的大きい(1.6-2.2倍程度) in vitro実験の結果、肝取り込みに主にOATP1B1が寄与することが示唆されている。 肝排泄過程にNTCP, MRP2, BCRPが関与。腎排泄過程には、OAT3が関与。 消化管吸収過程にBCRPが関与。
OATP1B3	*SLCO1B3*	Telmisartan	in vitro実験の結果、肝取り込みがOATP1B3選択的であることが示されている。 消化管、肝臓のUGTによる抱合代謝を受け、グルクロン酸としてほぼ胆汁排泄される。 臨床投与量の範囲内で、薬物動態の非線形性がみられている。
OAT1	*SLC22A6*	Acyclovir, Adefovir, Ganciclovir, Cidofovir	分泌クリアランスが腎クリアランス全体に占める割合が大きい。 in vitro実験の結果、OAT1選択的な取り込みを受ける。
OAT3	*SLC22A8*	Benzylpenicillin, Sitagliptin, Ciprofloxacin	分泌クリアランスが腎クリアランス全体に占める割合が大きい。 in vitro実験の結果、OAT3選択的な取り込みを受ける。
		Pravastatin, Rosuvastatin	腎クリアランスが全身クリアランスの3割程度を占める。OAT3選択的な基質。 腎クリアランスの算出により、OAT3の阻害効果は確認可能。
MATE1, MATE-2K, OCT2	*SLC47A1, SLC47A2, SLC22A2*	Metformin	OCT1, OCT2, MATEsの良好な基質。未変化体でほぼ腎排泄。 MATEs阻害時に、血中濃度上昇としては観察しにくく、probeとしての感度がよくない。 MATEs以外の腎排泄経路の存在が示唆。
		N-methylnicotinamide (NMN)	OCT1, OCT2, MATEsの良好な基質。未変化体でほぼ腎排泄。 MATEs阻害(pyrimethamine投与)時に、腎クリアランスの70%低下がみられており、probeとしての感度はよい。 内因性基質のため、外から投薬が必要ない。 血中濃度は、食事やcircadian rhythmの影響を受けるため、腎クリアランスとして評価する必要あり。

in vivo probe阻害剤

Transporter	Gene	Inhibitor	コメント
P-gp	*ABCB1*	Quinidine, Cyclosporin, Ranolazine, Amiodarone	CYP3A4に対する阻害効果は、P-gp阻害剤の中では弱い digoxinの血中濃度を1.5倍以上上昇させうる。 Cyclosporinは、OATPsの阻害剤でもあるので、注意を要する。
		Itraconazole, Clarithromycin, Verapamil	CYP3A4に対する阻害効果は、P-gp阻害剤の中では弱い digoxinの血中濃度を1.5倍以上上昇させうる。 Clarithromycinは、OATPsの阻害剤でもあるので、注意を要する。
BCRP	*ABCG2*	Curcumin	サプリメントであり、安全性は比較的高い 必要な投与量が2gと高い。 sulfasalazine以外に相互作用試験の適用例がない
		Eltrombopag	安全域が狭いので、注意が必要 rosuvastatin以外に相互作用試験の適用例がない
OATP1B1, OATP1B3	*SLCO1B1, SLCO1B3*	Cyclosporin A	安全域が狭いので、注意が必要 肝臓・消化管のCYP3A4や消化管のP-gpに対しても阻害効果を示す。
		Rifampicin	600mg単回経口投与により、十分にOATP1B1, 1B3の機能を阻害しうる。 これまでに健常人でのヒト試験の実績が多い。 代謝酵素やP-gpなどに対する阻害定数が大きく、生体内では阻害しないと考えられる。 複数回反復投与すると、CYP3A4, P-gpなどの発現上昇がみられる。
OAT1, OAT3	*SLC22A6, SLC22A8*	Probenecid	OAT1, OAT3両方共の強力な阻害剤。(ただし、OAT1, OAT3の分離評価はできない) これまでに健常人でのヒト試験の実績が多い。
MATE1, MATE2-K	*SLC47A1, SLC47A2*	Cimetidine	これまでに健常人でのヒト試験の実績が多い。 阻害強度から考えると、MATEsの完全な阻害は見込めず、部分的な阻害にとどまる。 報告されているcimetidineとの相互作用事例のうち、いくつかはMATEsで説明がつかず、未知の相互作用点がある可能性がある。
		Pyrimethamine	臨床投与量の範囲内で、MATEsを選択的に阻害可能。 日本では、単剤での承認薬がない。(スルファドキシンとの合剤のみ承認) 安全性に関してデータが少なく、情報が乏しい。

表5-5　トランスポーターの*in vitro* probe基質、阻害剤の例

in vitro probe基質

Transporter	Gene	Substrate	Km値[a]	コメント
P-gp	*ABCB1*	Digoxin	73-177 uM	OATP1B3基質
		Loperamide	(1.8-5.5 uM)	
		Quinidine	1.69 uM	
		Vinblastine	19-253 uM	MRP2基質
		Talinolol	(72 uM)	MRP2基質
		Fexofenadine	150 uM	OATPs, MRP2, MRP3基質
BCRP	*ABCG2*	Estrone-3-sulfate	2.3-13 uM	Caco-2のbasal側に取り込みトランスポーターが示唆, OATPs, NTCP基質
		Dantrolene		
		Daidzein		
		Genistein		
		Coumestrol		
OATP1B1, OATP1B3	*SLCO1B1, SLCO1B3*	Estradiol-17β-glucuronide	2.5-8.3 uM (1B1), 15.8-24.6 uM (1B3)	OATP1B1, 1B3両方の基質
		Estrone-3-sulfate	0.23-12.5 uM	OATP1B1選択的基質、阻害実験の際、全体的にKi値が大きく見積もられる傾向有り。
		Cholecystokinin octapeptide	3.8-16.5 uM	OATP1B3選択的基質
		Telmisartan	0.81 uM	OATP1B3選択的基質。吸着が大きく、実験系にalbuminの共存を考慮。
OAT1	*SLC22A6*	p-aminohippurate	4-20 uM	
		Adefovir	23.8-30 uM	
		Cidofovir	30-58 uM	
OAT3	*SLC22A8*	Benzylpenicillin	52 uM	OATPs, MRP2基質
		Estrone-3-sulfate	2.2-75 uM	OATP1B1, BCRP基質
		Pravastatin	27.2 uM	OATPs, MRP2基質
MATE1, MATE-2K	*SLC47A1, SLC47A2*	Tetraethylammonium (TEA)	220-380 uM (MATE1), 760-830 uM (MATE-2K)	OCTs基質
		Metformin	202-780 uM (MATE1), 1050-1980 uM (MATE-2K)	OCTs基質
		1-methyl-4-phenylpyridinium (MPP+)	100 uM (MATE1), 110 uM (MATE-2K)	OCTs基質
OCT2	*SLC22A2*	Tetraethylammonium (TEA)	33.8-76 uM	MATEs基質
		Metformin	680-3356 uM	MATEs基質
		1-methyl-4-phenylpyridinium (MPP+)	1.2-22.2 uM	MATEs基質

[a] ()内に示された数字は、Ki or IC50値

in vitro probe阻害剤

Transporter	Gene	Substrate	Ki or IC50値[b]	コメント
P-gp	*ABCB1*	Cyclosporin A	0.5-2.2 uM	MRP2, BCRP, NTCP, OATPs阻害剤
		Ketoconazole	1.2-6.3 uM	NTCP阻害剤
		Zosuquidar (LY335979)	0.024-0.07 uM	3 uMの利用で、選択的にP-gpを阻害できるとの報告あり (Mease K et al., J Pharm Sci., 101, 1888-1897 (2012)
		Quinidine	3.2-51.7 uM	OCT2, MATEs阻害剤
		Ritonavir	3.8-28 uM	OATPs阻害剤
		Tacrolimus	0.74 uM	OATPs阻害剤
		Valspodar (PSC833)	0.11 uM	MRP2阻害剤
		Verapamil	2.1-33.5 uM	OCTs, MATEs阻害剤
		Elacridar (GF120918)	0.027-0.44 uM	BCRP阻害剤
		Reserpine	1.4-11.5 uM	MRP2阻害剤
BCRP	*ABCG2*	Sulfasalazine	0.73 uM	細胞系の場合、細胞透過性が悪く濃度が達しない可能性あり。(膜ベシクル系では適用可)
		Elacridar (GF120918)	0.31 uM	P-gp阻害剤
		Fumitremorgin C	0.25-0.55 uM	1 uMの利用で、選択的にBCRPを阻害できるとの報告あり (Mease K et al., J Pharm Sci., 101, 1888-1897 (2012)
		Ko143	0.01 uM	
		Ko134	0.07 uM	
		noboviocin	0.063 - 0.095 uM	
OATP1B1, OATP1B3	*SLCO1B1, SLCO1B3*	Estradiol-17β-glucuronide	(2.5-8.3 uM (1B1), 15.8-24.6 uM (1B3))	MRP2, BCRP阻害剤
		Estrone-3-sulfate	0.2-0.79 uM (1B1), 97.1 uM (1B3)	阻害剤濃度の選択により、OATP1B1を選択的に阻害可能。BCRP, NTCP阻害剤
		Rifampicin	0.48-17 uM (1B1), 0.8-5 uM (1B3)	
		Rifamycin SV	0.17-2 uM (1B1), 3 uM (1B3)	
		Cyclosporin A	0.24-3.5 uM (1B1), 0.06-0.8 uM (1B3)	MDR1, MRP2、NTCP阻害剤
OAT1, OAT3	*SLC22A6, SLC22A8*	Probenecid	3.9-26 uM (OAT1), 1.3-9 uM (OAT3)	OATPs阻害剤
		Benzylpenicillin	1700 uM (OAT1), 52 uM (OAT3)	阻害剤濃度の選択により、OAT3のみを阻害可能。
MATE1, MATE-2K	*SLC47A1, SLC47A2*	Pyrimethamine	77 nM (MATE1), 46 nM (MATE-2K)	
		Cimetidine	1.1-3.8 uM (MATE1), 2.1-7.3 uM (MATE-2K)	OCTs阻害剤
OCT2	*SLC22A2*	Tetraethylammonium (TEA)	144 uM	MATEs基質
		1-methyl-4-phenylpyridinium (MPP+)	(1.2-22.2 uM)	MATEs基質

[b] ()内に示された数字は、Km値

III. 研究成果の刊行に関する一覧表と別刷

研究成果の刊行に関する一覧表

書籍

著者氏名	論文名	書籍全体の編集者名	書籍名	出版社名	出版地	出版年	ページ
該当なし							

雑誌

著者氏名	論文名	雑誌名	巻	ページ	刊行年
Kudo T, Hisaka A, Sugiyama Y, Ito K	Analysis of the repaglinide concentration increase produced by gemfibrozil and itraconazole based on the inhibition of the hepatic uptake transporter and metabolic enzymes	Drug Metab Dispos	41	362-371	2013
Sai K, Hanatani T, Azuma Y, Segawa K, Tohkin M, Omatsu H, Makimoto H, Hirai M, Saito Y	Development of a detection algorithm for statin-induced myopathy using electronic medical records	J Clin Pharm Ther	38	230-235	2013
Maeda K, Sugiyama Y	Transporter biology in drug approval: regulatory aspects	Mol Aspects Med	34	711-718	2013

1521-009X/41/2/362–371$25.00
DRUG METABOLISM AND DISPOSITION
http://dx.doi.org/10.1124/dmd.112.049460
Drug Metab Dispos 41:362–371, February 2013

Analysis of the Repaglinide Concentration Increase Produced by Gemfibrozil and Itraconazole Based on the Inhibition of the Hepatic Uptake Transporter and Metabolic Enzymes

Toshiyuki Kudo, Akihiro Hisaka, Yuichi Sugiyama, and Kiyomi Ito

Research Institute of Pharmaceutical Sciences, Musashino University, Tokyo, Japan (T.K., K.I.); Pharmacology and Pharmacokinetics, University of Tokyo Hospital, Tokyo, Japan (A.H.); and Sugiyama Laboratory, RIKEN Innovation Center, RIKEN Research Cluster for Innovation, Yokohama, Japan (Y.S.)

Received October 11, 2012; accepted November 8, 2012

ABSTRACT

The plasma concentration of repaglinide is reported to increase greatly when given after repeated oral administration of itraconazole and gemfibrozil. The present study analyzed this interaction based on a physiologically based pharmacokinetic (PBPK) model incorporating inhibition of the hepatic uptake transporter and metabolic enzymes involved in repaglinide disposition. Firstly, the plasma concentration profiles of inhibitors (itraconazole, gemfibrozil, and gemfibrozil glucuronide) were reproduced by a PBPK model to obtain their pharmacokinetic parameters. The plasma concentration profiles of repaglinide were then analyzed by a PBPK model, together with those of the inhibitors, assuming a competitive inhibition of CYP3A4 by itraconazole, mechanism-based inhibition of CYP2C8 by gemfibrozil glucuronide, and inhibition of organic anion transporting polypeptide (OATP) 1B1 by gemfibrozil and its glucuronide. The plasma concentration profiles of repaglinide were well reproduced by the PBPK model based on the above assumptions, and the optimized values for the inhibition constants (0.0676 nM for itraconazole against CYP3A4; 14.2 μM for gemfibrozil against OATP1B1; and 5.48 μM for gemfibrozil glucuronide against OATP1B1) and the fraction of repaglinide metabolized by CYP2C8 (0.801) were consistent with the reported values. The validity of the obtained parameters was further confirmed by sensitivity analyses and by reproducing the repaglinide concentration increase produced by concomitant gemfibrozil administration at various timings/doses. The present findings suggested that the reported concentration increase of repaglinide, suggestive of synergistic effects of the coadministered inhibitors, can be quantitatively explained by the simultaneous inhibition of the multiple clearance pathways of repaglinide.

Introduction

Repaglinide is one of the short-acting meglitinide analogs that reduce blood glucose concentrations by enhancing glucose-stimulated insulin secretion from pancreatic beta cells (Fuhlendorff et al., 1998). It has been reported that the plasma concentration of repaglinide after an oral dose was dramatically increased when it was given following repeated oral administration of itraconazole (ICZ; 100 mg) and gemfibrozil (GEM; 600 mg) twice a day for 3 days in healthy volunteers [the area under the concentration-time curve (AUC) of repaglinide was increased 1.4-, 8.1-, and 19.4-fold by ICZ, GEM, and both, respectively] (Niemi et al., 2003a). The major route of repaglinide elimination from the body is active uptake from blood into hepatocytes by an uptake transporter, organic anion transporting polypeptide (OATP) 1B1, followed by biotransformation by cytochrome P450 (P450) enzymes (CYP3A4 and CYP2C8) into several metabolites (van Heiningen et al., 1999; Bidstrup et al., 2003; Kajosaari et al., 2005a; Niemi et al., 2005; Kalliokoski et al., 2008). Therefore, the above interactions possibly resulted from inhibitions of OATP1B1, CYP3A4, and CYP2C8.

The plasma repaglinide concentration after oral administration in humans has been reported to be affected by genetic polymorphisms of OATP1B1 and CYP2C8: for OATP1B1, subjects with the 521CC

This work was supported by JSPS KAKENHI Grant [23590204].
dx.doi.org/10.1124/dmd.112.049460.

ABBREVIATIONS: AUC, area under the concentration-time curve; β, CL_{int} divided by (CL_{int} + PS_{eff}); C_b, concentrations in the blood compartment; C_e, concentration in the liver extracellular space compartment; C_h, concentrations in the liver compartment; CL_h, hepatic clearance; CL_{int}, intrinsic metabolic clearance; $CL_{int,all}$, overall intrinsic clearance; $CL_{int,h}$, hepatic intrinsic clearance; CL_{NH}, non-hepatic clearance; cLogP, logarithm of the computer-calculated partition coefficient between *n*-octanol and water; CL_{tot}, total body clearance; P450, cytochrome P450; F_a, fraction absorbed; f_b, blood unbound fraction; f_e, urinary excretion ratio of parent drug; F_g, intestinal availability; F_h, hepatic availability; f_h, unbound fraction in the liver; fm_{2C8}, fraction metabolized by CYP2C8; GEM, gemfibrozil; GEM-glu, gemfibrozil glucuronide; IC_{50}, half maximal inhibitory concentration; ICZ, itraconazole; k_{12}, transfer rate constant from the blood compartment to the peripheral compartment; k_{21}, transfer rate constant from the peripheral compartment to the blood compartment; k_a, absorption rate constant; $k_{deg,2C8}$, the first-order rate constant for degradation of CYP2C8; $K_{i,1B1}$, inhibition constant for hepatic uptake; $K_{i,3A4}$, the inhibition constant for CYP3A4-mediated hepatic metabolism; $Ki_{,app,2C8}$, the apparent inhibition constant for CYP2C8-mediated hepatic metabolism; $k_{inact,2C8}$, the maximum inactivation rate constant for CYP2C8-mediated hepatic metabolism; K_p, liver-to-plasma concentration ratio; Lag, lag time for absorption; OATP, organic anion transporting polypeptide; PBPK, physiologically based pharmacokinetic; PS_{eff}, intrinsic clearance for the efflux from hepatocytes to blood; PS_{inf}, intrinsic clearance for hepatic uptake from blood; Q_h, hepatic blood flow; R2C8, inhibition ratio of CYP2C8; R3A4, inhibition ratio of CYP3A4; R_b, blood-to-plasma concentration ratio; R_{inf}, inhibition ratio of hepatic uptake; V_b, distribution volume in the blood compartment; V_e, volume of the liver extracellular space; V_h, volume of liver; X_{sub}, amount in the peripheral compartment.

genotype have a significantly higher (1.7- to 2.9-fold) repaglinide AUC than those with the wild type (521TT) (Niemi et al., 2005; Kalliokoski et al., 2008); for CYP2C8, subjects with the CYP2C8*1/*3 genotype have a significantly lower (0.5-fold) repaglinide AUC than those with wild type (*1/*1) (Niemi et al., 2003b, 2005). On the other hand, there was no difference in the AUC of repaglinide between the subjects with the CYP3A4 *1/*18 genotype and those with the wild type (*1/*1) (Ruzilawati and Gan, 2010).

The coadministered inhibitors of OATP1B1, CYP2C8, and CYP3A4 have also been reported to affect the disposition of repaglinide: the AUC of oral repaglinide was significantly increased by coadministration of clarithromycin (1.4-fold) (Niemi et al., 2001) and cyclosporine (2.4-fold) (Kajosaari et al., 2005b), which are known to inhibit both OATP1B1 and CYP3A4; coadministration of telithromycin and trimethoprim, an inhibitor of CYP3A4 and CYP2C8, respectively, increased the AUC of oral repaglinide by 1.8-fold (Kajosaari et al., 2006) and 1.6-fold (Niemi et al., 2004), respectively. It has also been reported that repeated administration of rifampicin, an inducer of P450 enzymes, including CYP3A4 and CYP2C8, significantly reduced the AUC of oral repaglinide (0.2- or 0.4-fold) (Niemi et al., 2000; Bidstrup et al., 2004).

ICZ is known to be a potent reversible inhibitor of CYP3A4. In in vitro studies using human liver microsomes, ICZ strongly inhibited the biotransformation of substrates of CYP3A4, such as midazolam, quinidine and testosterone (von Moltke et al., 1996; Galetin et al., 2005). The AUCs of oral triazolam and midazolam, both eliminated from the body mainly by CYP3A4-mediated metabolism, were significantly increased when coadministered with ICZ (200 mg p.o., once a day, for 4 days) by 27- and 6.2-fold, respectively (Varhe et al., 1994; Backman et al., 1998).

GEM inhibited the CYP2C8-mediated metabolism of paclitaxel and cerivastatin in human liver microsomes without affecting the CYP3A4-mediated hydroxylation of testosterone (Wang et al., 2002; Shitara et al., 2004). It was also found that GEM glucuronide (GEM-glu) is a mechanism-based inhibitor of CYP2C8 (Ogilvie et al., 2006), and this was supported by a persistent interaction between GEM and repaglinide in vivo (Tornio et al., 2008). Both GEM and GEM-glu are also reported to inhibit OATP1B1 in in vitro studies using human hepatocytes and OATP1B1-expressing cells (Shitara et al., 2004; Nakagomi-Hagihara et al., 2007). The AUCs of oral pravastatin and rosuvastatin, mainly taken up into the liver by OATP1B1 and excreted into bile in unchanged forms, were significantly increased when coadministered with GEM (600 mg p.o., twice a day, for 3 days) by 2- and 1.9-fold, respectively (Kyrklund et al., 2003; Schneck et al., 2004). In addition, the AUC of cerivastatin, a substrate of OATP1B1 and CYP2C8, was significantly increased when coadministered with GEM (600 mg p.o., twice a day, for 3 days) by 4.4-fold (Backman et al., 2002), and this was suggested to result from the inhibition of OATP1B1 and CYP2C8 by both GEM and GEM-glu (Shitara et al., 2004).

Taken together, these pieces of evidence support the hypothesis that the reported drastic increase in the AUC of repaglinide resulted from the inhibition of OATP1B1, CYP3A4, and CYP2C8 by ICZ or GEM. The present study aimed to analyze this interaction quantitatively using a physiologically based pharmacokinetic (PBPK) model for all the compounds (repaglinide, GEM, and GEM-glu) involved in the interaction. Although PBPK models have been used for the quantitative prediction of the degree of drug-drug interaction involving metabolic enzymes (Kanamitsu et al., 2000; Ito et al., 2003; Kato et al., 2008; Zhang et al., 2009; Rowland-Yeo et al., 2010; Zhao et al., 2012) and also for describing the disposition of a drug transporter substrate pravastatin (Watanabe et al., 2009), only "static" approaches have been used for the interactions at drug transporters (Hinton et al., 2008; Yoshida et al., 2012), with no reports on the application of PBPK modeling to the best of our knowledge. In the present study, we investigated whether the increase in repaglinide AUC by ICZ and GEM can be quantitatively explained based on the clearance concept and a PBPK model incorporating the inhibition of both the hepatic uptake transporter and metabolic enzymes.

Materials and Methods

Calculation of Pharmacokinetic Parameters for Repaglinide

The urinary excretion of repaglinide is reported to be negligible (0.1%) after its intravenous administration to healthy volunteers (van Heiningen et al., 1999). Therefore, the total body clearance (CL_{tot}) was assumed to be equal to the hepatic clearance (CL_h) and the hepatic availability (F_h) was calculated as $1 - CL_h/Q_h$, where Q_h represents the hepatic blood flow (86.9 l/h) (Watanabe et al., 2009). As the bioavailability (0.625) estimated from an oral/intravenous administration study (Hatorp, 2002) exceeds the estimated F_h of 0.40 (0.25–0.52 using the Q_h of 70–110 l/h), a product of F_a and F_g, where F_a and F_g represent the fraction absorbed and the intestinal availability, respectively, was assumed to be unity. Thus, the overall intrinsic clearance ($CL_{int,all}$) for hepatic elimination of repaglinide, multiplied by the blood unbound fraction (f_b), was calculated by the following equation using the AUC values reported in the interaction study with ICZ/GEM (4.74, 6.66, 38.3, and 91.5 ng/h per ml for control, +ICZ, +GEM, and +ICZ+GEM, respectively) (Niemi et al., 2003a).

$$f_b \cdot CL_{int,all} = \frac{Dose}{AUC} \quad (1)$$

where Dose is the oral dose of repaglinide (0.25 mg for all conditions).

Estimation of the Inhibition Ratio of Intrinsic Clearances for Each Process Based on the AUC Increase produced by ICZ and GEM

The $CL_{int,all}$ calculated above is expressed as follows (Shitara et al., 2006):

$$CL_{int,all} = \frac{PS_{inf} \cdot CL_{int}}{CL_{int} + PS_{eff}} = \frac{PS_{inf} \cdot CL_{int}/PS_{eff}}{CL_{int}/PS_{eff} + 1} = \frac{PS_{inf} \cdot \gamma}{1+\gamma} = PS_{inf} \cdot \beta \quad (2)$$

where PS_{inf} and PS_{eff} represent the intrinsic clearance for hepatic uptake from blood and the efflux from hepatocytes to blood, respectively; γ is defined as CL_{int}/PS_{eff}; β, defined as $CL_{int}/(CL_{int}+PS_{eff})$, can be used for evaluating the rate-limiting process of hepatic intrinsic clearance. CL_{int} represents the intrinsic clearance for hepatic metabolism mediated by CYP2C8 and CYP3A4, which can be expressed as follows using the fraction metabolized by CYP2C8 (fm_{2C8}):

$$CL_{int} = CL_{int2C8} + CL_{int3A4} = fm_{2C8} \times CL_{int} + (1 - fm_{2C8}) CL_{int} \quad (3)$$

For the control (administration of repaglinide alone), the following equations can be derived from the above equations:

$$AUC_{cont} = \frac{Dose_{cont}}{f_b \cdot PS_{inf} \times \frac{\gamma}{1+\gamma}} \quad (4)$$

assuming that ICZ inhibits CYP3A4, the following equations can be derived for +ICZ (coadministration of ICZ) condition:

$$AUC_{+ICZ} = \frac{Dose_{+ICZ}}{f_b \cdot PS_{inf} \times \frac{\gamma_{+ICZ}}{1+\gamma_{+ICZ}}} \quad (5)$$

$$\gamma_{+ICZ} = fm_{2c8} \times \gamma + (1 - fm_{2c8}) \times \gamma \times R3A4 \quad (6)$$

where R3A4 represents the inhibition ratio of CYP3A4 by ICZ [$CL_{int,3A4}$(+ICZ)/$CL_{int,3A4}$(control)]. Assuming that GEM (and its glucuronide) inhibits both OATP1B1 and CYP2C8, the following equations can be derived for the +GEM (coadministration of GEM) condition:

$$AUC_{+GEM} = \frac{Dose_{+GEM}}{R_{inf} \times f_b \cdot PS_{inf} \times \frac{\gamma_{+GEM}}{1+\gamma_{+GEM}}} \quad (7)$$

$$\gamma_{+GEM} = fm_{2c8} \times \gamma \times R2C8 + (1 - fm_{2c8}) \times \gamma \quad (8)$$

where R_{inf} and R2C8 represents the inhibition ratio of hepatic uptake and CYP2C8, respectively, by GEM [PS_{inf}(+GEM)/PS_{inf}(control) and $CL_{int,2C8}$(+GEM)/$CL_{int,2C8}$(-control), respectively]. Finally, the AUC and R values can be expressed as follows for the +ICZ+GEM (coadministration of both ICZ and GEM) condition:

$$AUC_{+ICZ+GEM} = \frac{Dose_{+ICZ+GEM}}{R_{inf} \times f_b \cdot PS_{inf} \times \dfrac{\gamma_{+ICZ+GEM}}{1 + \gamma_{+ICZ+GEM}}} \quad (9)$$

$$\gamma_{+ICZ+GEM} = fm_{2C8} \times \gamma \times R2C8 + (1 - fm_{2C8}) \times \gamma \times R3A4 \quad (10)$$

The observed AUC values for the four conditions (control, +ICZ, +GEM, and +ICZ +GEM) were analyzed by the above equations using a multipurpose nonlinear least-squares fitting computer program Napp (version 2.26) (Hisaka and Sugiyama, 1998) to obtain the optimized values for R_{inf}, R2C8, R3A4, and fm_{2C8}, fixing the $f_b \cdot PS_{inf}$ value at 100 l/h.

Fitting Analyses of the Blood Concentration-Time Profiles of Inhibitors (ICZ, GEM, and GEM-glu) Based on a Simple PBPK Model

ICZ. A simple PBPK model for ICZ disposition, consisting of a blood compartment, a gastrointestinal compartment, and a liver compartment, was constructed as shown in Fig. 1A. According to this model, the concentration profile of ICZ can be expressed by the following differential equations:

$$V_{b,icz}\frac{dC_{b,icz}}{dt} = Q_h\frac{R_{b,icz}}{K_{p,icz}}C_{h,icz} - Q_h \cdot C_{b,icz} \quad (11)$$

$$V_h\frac{dC_{h,icz}}{dt} = Q_h \cdot C_{b,icz} - Q_h\frac{R_{b,icz}}{K_{p,icz}}C_{h,icz} - f_{h,icz} \cdot CL_{int,icz} \cdot C_{h,icz} + k_{a,icz} \cdot F_a F_{g,icz} \cdot Dose_{icz} \cdot \exp(-k_{a,icz} \cdot t) \quad (12)$$

where C_b and C_h represent the concentrations in the blood and liver compartments, respectively; V_b represents the distribution volume in the blood compartment; V_h represents the volume of liver; k_a represents the absorption rate constant; R_b represents the blood-to-plasma concentration ratio; K_p represents the liver-to-plasma concentration ratio; and f_h represents the unbound fraction in the liver. The subscript icz after each parameter indicates the parameters for ICZ.

Because the concentration profile of ICZ was not shown in the interaction study with repaglinide (Niemi et al., 2003a), the values of $V_{b,icz}$, $k_{a,icz}$, and $CL_{int,icz}$ were optimized by fitting analyses based on the concentration profile reported in another paper (Jaakkola et al., 2005). The dose was set at 100,000 μg (Niemi et al., 2003a; Jaakkola et al., 2005), and values of Q_h = 86.9 l/h and

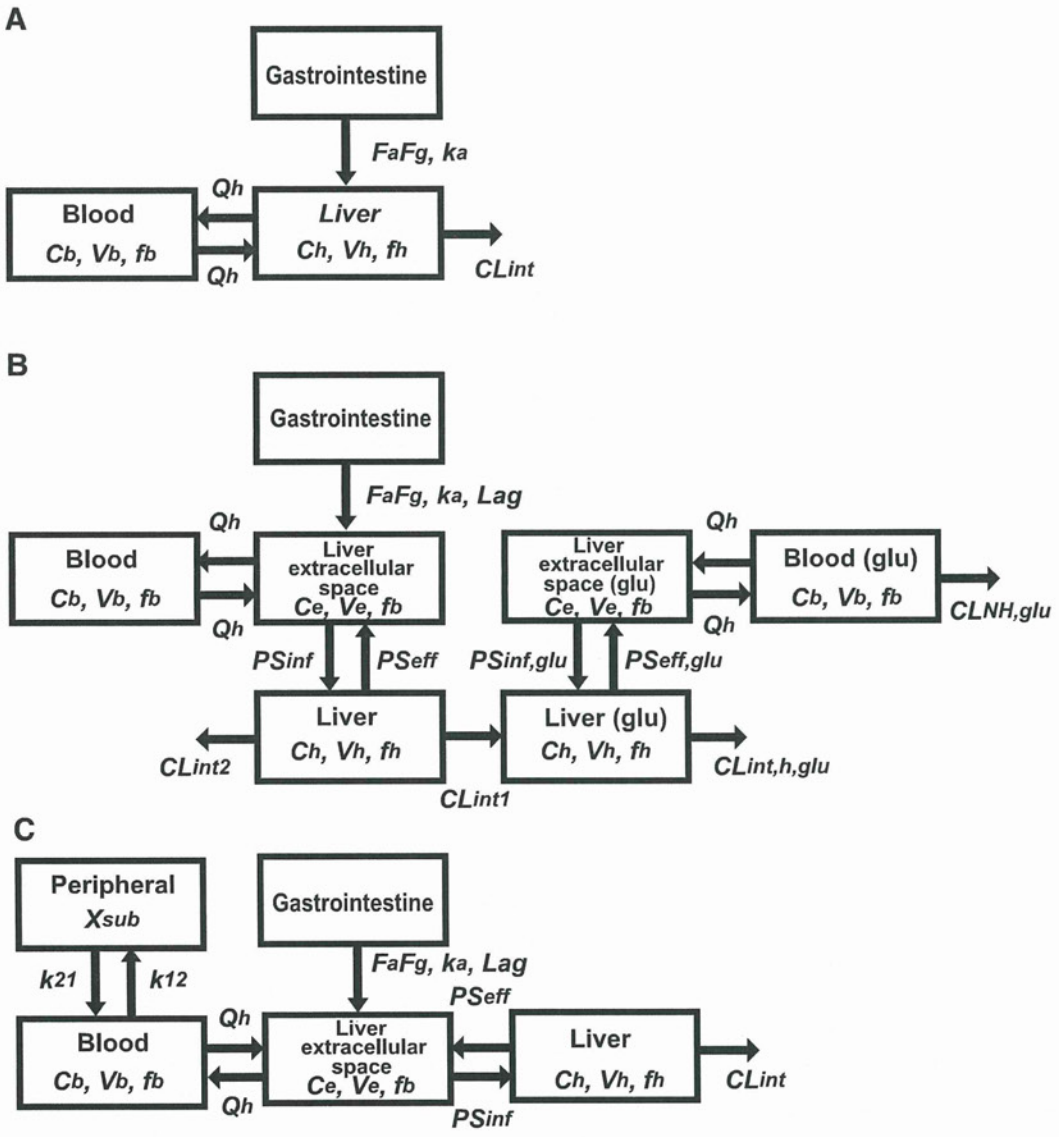

Fig. 1. Simple PBPK models for ICZ (A), GEM/GEM-glu (B), and repaglinide (C).

V_h=1.22 l were used for physiologic parameters (Watanabe et al., 2009). The F_aF_g was estimated by a similar method as that for repaglinide described above using the values of CL_{tot} and bioavailability (Table 1), The f_h value was calculated based on the following equation (Poulin and Theil, 2002):

$$f_p/f_h = 0.5 \times (f_p + 1) \quad (13)$$

where f_p represents the unbound fraction in the plasma. The K_p value was calculated as follows (Poulin and Theil, 2002):

$$K_p = (P \times 0.02289 + 0.72621)/(P \times 0.001719 + 0.960581) \times f_p/f_h \quad (14)$$

$$P = 10^{cLogP} \quad (15)$$

where cLogP represents the logarithm of the computer-calculated partition coefficient between *n*-octanol and water. The initial ICZ concentration in the blood compartment ($C_{b,0}$) after 3 days of repeated oral administration was obtained from the reported concentration profile (Jaakkola et al., 2005). The initial ICZ concentration in the liver compartment ($C_{h,0}$) was assumed to be equal to $C_{b,0} \times K_p / R_b$.

GEM and GEM-glu. A simple PBPK model constructed for GEM and GEM-glu disposition, consisting of a blood compartment, a gastrointestinal compartment, a liver extracellular space compartment, and a liver compartment for GEM and a blood compartment, a liver extracellular space compartment, and a liver compartment for GEM-glu, is shown in Fig. 1B. According to this model, the concentration profiles of GEM and GEM-glu can be expressed by the following differential equations:

$$V_{b,gem}\frac{dC_{b,gem}}{dt} = Q_h \cdot C_{e,gem} - Q_h \cdot C_{b,gem} \quad (16)$$

$$\begin{aligned} V_e\frac{dC_{e,gem}}{dt} = {} & Q_h \cdot C_{b,gem} - Q_h \cdot C_{e,gem} - f_{b,gem} \cdot PS_{inf,gem} \cdot C_{e,gem} \\ & + f_{h,gem} \cdot PS_{eff,gem} \cdot C_{h,gem} \\ & + k_{a,gem} \cdot F_aF_{g,gem} \cdot Dose_{gem} \cdot \exp(-k_{a,gem}(t - Lag_{gem})) \end{aligned} \quad (17)$$

TABLE 1

Pharmacokinetic parameters for inhibitors

Parameters	Units	Values	Sources
For ICZ			
Bioavailability		0.55	Thummel et al., 2011
CL_{tot} (plasma)	l/h	21.4	Thummel et al., 2011
CL_{tot} (blood)	l/h	36.9	CL_{tot} (plasma) / R_b
f_e		< 0.01	Thummel et al., 2011
CL_h (blood)	l/h	36.9	Assuming $CL_r = 0$
F_h		0.575	1-CL_h/Q_h
F_aF_g		0.957	Bioavailability / F_h
f_p		0.002	Thummel et al., 2011
R_b		0.58	Kato et al., 2008
cLogP		6.05	Calculated by using ChemDraw Ultra 7.0
K_p		6.67	Eq. 14
f_h		0.000300	Eq. 13
Dose	μg	100,000	Niemi et al., 2003a
k_a	h^{-1}	0.121 ± 0.037	*
V_b	l	59.2 ± 36.2	*
CL_{int}	l/h	14,700 ± 2,600	*
$C_{b,0}$	μg/l	98	Jaakkola et al., 2005
$C_{h,0}$	μg/l	1,131	Assuming $C_{h,0} = C_{b,0} \times K_p / R_b$
For GEM			
Bioavailability		0.98	Thummel et al., 2011
CL_{tot} (plasma)	l/h	7.14	Thummel et al., 2011
CL_{tot} (blood)	l/h	12.9	CL_{tot} (plasma) / R_b
f_e		< 0.01	Thummel et al., 2011
CL_h (blood)	l/h	12.9	Assuming $CL_r = 0$
F_h		0.85	1-CL_h/Q_h
F_aF_g		1	Bioavailability > F_h
f_p		0.0065	Shitara et al., 2004
f_b		0.012	f_p / R_b
R_b		0.55	Kilford et al., 2009
f_h		0.013	Eq. 13
Dose	μg	600,000	Niemi et al., 2003a
k_a	h^{-1}	3.13 ± 0.36	*
Lag	h	0.25	Estimated to fit the blood concentration profile of GEM
V_b	l	13.3 ± 8.6	*
CL_{int1}	l/h	199 ± 506	*
CL_{int2}	l/h	32.6	$CL_{int,gem1}$ / $CL_{int,gem2}$ = 6.1
PS_{inf}	l/h	8,470	$CL_{int,all} \times 10$
PS_{eff}	l/h	2,010 ± 5,110	*
For GEM-glu			
f_p		0.115	Shitara et al., 2004
f_b		0.209	f_p / R_b
R_b		0.55	Assumed to be the same as GEM
f_h		0.206	Eq. 13
V_b	l	5.2	Blood volume
CL_{NH}	l/h	1.57	Glomerular filtration rate × $f_{b,glu}$
$CL_{int,h}$	l/h	12.5 ± 2.7	*
PS_{inf}	l/h	469	Assuming $f_b \cdot PS_{inf,gem} = f_b \cdot PS_{inf,glu}$
PS_{eff}	l/h	100 ± 20	*

* Optimized by fitting analysis.

$$V_h\frac{dC_{h,gem}}{dt} = f_{b,gem}\cdot PS_{\inf,gem}\cdot C_{e,gem} - f_{h,gem}\cdot PS_{eff,gem}\cdot C_{h,gem} \quad (18)$$
$$(f_{h,gem}\cdot CL_{int1} + f_{h,gem}\cdot CL_{int2})C_{h,gem}$$

$$V_{b,glu}\frac{dC_{b,glu}}{dt} = Q_h\cdot C_{e,glu} - Q_h\cdot C_{b,glu} - CL_{NH,glu}\cdot C_{b,glu} \quad (19)$$

$$V_e\frac{dC_{e,glu}}{dt} = Q_h\cdot C_{b,glu} - Q_h\cdot C_{e,glu} - f_{b,glu}\cdot PS_{\inf,glu}\cdot C_{e,glu} + f_{h,glu}\cdot PS_{eff,glu}\cdot C_{h,glu} \quad (20)$$

$$V_h\frac{dC_{h,glu}}{dt} = f_{h,gem}\cdot CL_{int1}\cdot C_{h,gem} + f_{b,glu}\cdot PS_{\inf,glu}\cdot C_{e,glu} - f_{h,glu}\cdot PS_{eff,glu}\cdot C_{h,glu} - f_{h,glu}\cdot CL_{int,h,glu}\cdot C_{h,glu} \quad (21)$$

where V_e represents the volume of the liver extracellular space (0.469 l) (Watanabe et al., 2009); Lag represents the lag time for absorption of GEM; CL_{int1} and CL_{int2} were defined as the hepatic intrinsic clearances for glucuronidation and other metabolic pathway(s), respectively, for GEM; CL_{NH} represents the nonhepatic clearance for elimination of GEM-glu from the blood compartment; $CL_{int,h}$ represents the hepatic intrinsic clearance for elimination of GEM-glu from the liver compartment. The subscripts gem and glu after each parameter indicate the parameters for GEM and GEM-glu, respectively.

Because the concentration profiles of GEM and GEM-glu were not shown in the interaction study with repaglinide (Niemi et al., 2003a), the values of the pharmacokinetic parameters for GEM and GEM-glu were estimated based on their concentration profiles after repeated oral administration of GEM according to the same dosage schedule, as reported in another paper (Tornio et al., 2008). The dose was set at 600,000 μg (Niemi et al., 2003a; Tornio et al., 2008), and the F_aF_g for GEM was estimated by a similar method as that for repaglinide described above using the values of CL_{tot} and bioavailability (Table 1). The CL_{int1}/CL_{int2} ratio was fixed at 6.1 (= 0.86/0.14) because the fraction of GEM metabolized by the UDP-glucuronosyltransferase is reported to be 0.86 (Kilford et al., 2009). The $PS_{inf,gem}$ was assumed to be equal to 10-fold the value of $CL_{int,all}$ for GEM that was calculated by Eq. 1 using the reported AUC value (Tornio et al., 2008); the $PS_{inf,glu}$ was calculated based on an assumption that $fb\cdot PS_{inf,glu}$ was equal to $fb\cdot PS_{inf,gem}$; the $CL_{NH,glu}$ was assumed to be equal to the value of the glomerular filtration rate (Davies and Morris, 1993) multiplied by $f_{b,glu}$. Initially, the GEM blood concentration profile was fitted to Eq. 16 based on the simultaneous analysis of Eqs. 16–18 to obtain the optimized values of $k_{a,gem}$, $V_{b,gem}$, $PS_{eff,gem}$, and CL_{int1}. Then, fixing the above parameters for GEM at the optimized values, the GEM-glu blood concentration profile was fitted to Eq. 19 based on the simultaneous analysis of Eqs. 19–21 to obtain the optimized values of $PS_{eff,glu}$ and $CL_{int,h,glu}$.

Fitting Analyses of Repaglinide Concentration Profiles Based on a Simple PBPK Model

A simple PBPK model constructed for repaglinide disposition, consisting of a blood compartment, a gastrointestinal compartment, a peripheral compartment, a liver extracellular space compartment, and a liver compartment, is shown in Fig. 1C. According to this model, the concentration profile of repaglinide can be expressed by the following differential equations considering the inhibition of hepatic uptake by GEM and GEM-glu, a mechanism-based inhibition of CYP2C8 by GEM-glu and a competitive inhibition of CYP3A4 by ICZ:

$$V_{b,s}\frac{dC_{b,s}}{dt} = Q_h\cdot C_{e,s} - Q_h\cdot C_{b,s} - k_{12,s}\cdot V_{b,s}\cdot C_{b,s} + k_{21,s}\cdot X_{sub} \quad (22)$$

$$V_e\frac{dC_{e,s}}{dt} = Q_h\cdot C_{b,s} - Q_h\cdot C_{e,s} - \frac{f_{b,s}\cdot PS_{inf,s}}{1+\frac{f_{b,gem}\cdot C_{e,gem}}{K_{i,1B1,gem}}+\frac{f_{b,glu}\cdot C_{e,glu}}{K_{i,1B1,glu}}}C_{e,s} + f_{h,s}\cdot PS_{eff,s}\cdot C_{h,s} + k_{a,s}\cdot F_aF_{g,s}\cdot Dose_s \cdot \exp(-k_{a,s}(t-Lag_s)) \quad (23)$$

$$V_h\frac{dC_{h,s}}{dt} = \frac{f_{b,s}\cdot PS_{inf,s}}{1+\frac{f_{b,gem}\cdot C_{e,gem}}{K_{i,1B1,gem}}+\frac{f_{b,glu}\cdot C_{e,glu}}{K_{i,1B1,glu}}}C_{e,s} - f_{h,s}\cdot PS_{eff,s}\cdot C_{h,s} - f_{h,s}\cdot CL_{int,s}\left\{fm_{2C8}\cdot RE_{act,2C8} + \frac{1-fm_{2C8}}{1+\frac{f_{h,icz}\cdot C_{h,icz}}{K_{i,3A4,icz}}}\right\}C_{h,s} \quad (24)$$

$$\frac{dX_{sub}}{dt} = k_{12,s}\cdot V_{b,s}\cdot C_{b,s} - k_{21,s}\cdot X_{sub} \quad (25)$$

where the subscript s after each parameter indicates the parameters for repaglinide; X_{sub} represents the amount of repaglinide in the peripheral compartment; k_{12} and k_{21} represent the transfer rate constant from the blood compartment to the peripheral compartment and that from the peripheral compartment to the blood compartment, respectively; $K_{i,1B1}$ and $K_{i,3A4}$ represent the inhibition constant for hepatic uptake and that for CYP3A4-mediated hepatic metabolism, respectively. It was assumed that the inhibition of hepatic uptake and metabolism depends on the inhibitor concentration in the liver extracellular space compartment (C_e) and that in the liver compartment (C_h), respectively. Lag for repaglinide was assumed in the present analysis to include the 1-hour lag time between the doses of ICZ/GEM and repaglinide (Niemi et al., 2003a).

The differential equation for $REact_{2C8}$, the fraction of active CYP2C8, can be expressed as follows considering the mechanism-based inhibition by GEM-glu:

$$\frac{dRE_{act,2C8}}{dt} = -\frac{k_{inact,2C8}\cdot RE_{act,2C8}\cdot f_{h,glu}\cdot C_{h,glu}}{K_{i,app,2C8}+f_{h,glu}\cdot C_{h,glu}} + k_{deg,2C8}(1-RE_{act,2C8}) \quad (26)$$

where $k_{inact,2C8}$ and $K_{i,app,2C8}$ represent the maximum inactivation rate constant and the apparent inhibition constant, respectively, and $k_{deg,2C8}$ represents the first-order rate constant for degradation of CYP2C8.

The repaglinide blood concentration profiles for the four conditions (control, +ICZ, +GEM, and +ICZ+GEM) were fitted to Eq. 22 based on the simultaneous analysis of Eqs. 11, 12 and Eqs. 16–26 to obtain the optimized values of $k_{a,s}$, Lag_s, $V_{b,s}$, $f_{b,s}\cdot PS_{inf,s}$, $f_{h,s}\cdot CL_{int,s}$, $k_{12,s}$, $k_{21,s}$, $K_{i,3A4,icz}$, and $K_{i,1B1,gem}$. The dose of repaglinide was set at 250 μg, which is the oral dose used in the reported interaction study (Niemi et al., 2003a); the values of $K_{i,app,2C8}$, $k_{inact,2C8}$, and $k_{deg,2C8}$ were fixed at the reported values (20 μM, 12.6 h^{-1} and 0.030 h^{-1}, respectively) (Ogilvie et al., 2006; Yang et al., 2008); the ratio of $K_{i,1B1,glu}/K_{i,1B1,gem}$ was fixed at the mean of the reported values obtained in in vitro uptake studies using human hepatocytes and OATP1B1-expressing cells (0.385) (Shitara et al., 2004; Nakagomi-Hagihara et al., 2007); the values of $PS_{eff,s}$ was calculated as the geometric mean of the reported intrinsic clearances for passive diffusion of repaglinide into human and rat hepatocytes (Yabe et al., 2011; Ménochet et al., 2012; Jones et al., 2012) (Table 2). The PK parameters for ICZ, GEM, and GEM-glu were fixed at the values obtained by the above-mentioned analyses of respective concentration profiles (Table 1).

Simulation of the Repaglinide Concentration Profiles in Other Interaction Studies with GEM

Simulation studies were performed to investigate whether the repaglinide concentration increase produced by concomitant GEM administration at various timing/doses, reported in other papers, can be reproduced using the same PBPK model (Figs. 1, B and C, Eqs. 16–26) together with the parameters estimated in the present study (Table 2). The following three studies were investigated:

Report 1: repaglinide was taken 1, 24, 48, or 96 hours after the last administration of gemfibrozil (600 mg p.o., twice a day, for 3 days) (Backman et al., 2009).

Report 2: repaglinide was taken 0, 1, 3, or 6 hours after a single administration of gemfibrozil (600 mg p.o.) (Honkalammi et al., 2011).

Report 3: repaglinide was taken 1 hour after the last administration of gemfibrozil (30, 100, or 600 mg p.o., twice a day, for 3 days) (Honkalammi et al., 2012).

TABLE 2

Pharmacokinetic parameters for repaglinide and inhibition parameters

Parameters	Units	Values	Sources
Bioavailability		0.625	Hatorp, 2002
CL_{tot} (plasma)	l/h	32.6	Hatorp, 2002
CL_{tot} (blood)	l/h	52.6	CL_{tot} (plasma) / R_b
f_e		0.001	van Heiningen et al., 1999
CL_h (blood)	l/h	52.6	Assuming $CL_r = 0$
F_h		0.40	$1\text{-}CL_h/Q_h$
F_aF_g		1	Bioavailability > F_h
f_p		0.015	Hatorp, 2002
f_b		0.025	f_p / R_b
R_b		0.6	van Heiningen et al., 1999
Dose	μg	250	Niemi et al., 2003a
k_a	h^{-1}	4.51 ± 1.87	*
Lag	h	1.20 ± 0.06	*
V_b	l	8.38 ± 9.02	*
$f_h \cdot CL_{int}$	l/h	5.63 ± 4.88	*
$f_b \cdot PS_{inf}$	l/h	192 ± 127	*
$f_h \cdot PS_{eff}$	l/h	15.4	Yabe et al., 2011; Ménochet et al., 2012; Jones et al., 2012
k_{12}	h^{-1}	2.62 ± 3.60	*
k_{21}	h^{-1}	1.23 ± 0.30	*
fm_{2C8}		0.801 ± 0.049	*
$K_{i,3A4,icz}$	μg/l	0.0477 ± 0.0365	*
$K_{i,app,2C8}$	μM	20	Ogilvie et al., 2006
$k_{inact,2C8}$	h^{-1}	12.6	Ogilvie et al., 2006
$k_{deg,2C8}$	h^{-1}	0.03013	Yang et al., 2008
$K_{i,1B1,gem}$	μg/l	3,560 ± 2,530	*
$K_{i,1B1,glu}/K_{i,1B1,gem}$		0.385	Shitara et al., 2004; Nakagomi-Hagihara et al., 2007

* Optimized by fitting analysis.

Analysis

A multipurpose nonlinear least-squares fitting computer program Napp (version 2.26) (Hisaka and Sugiyama, 1998) was used for all the fitting and simulation analyses. The differential equations were numerically solved by using the Runge-Kutta-Fehlberg method. The fitting analysis was carried out based on a nonlinear least-squares procedure with a weight value fixed at 1.

Results

Analysis of the Increased Repaglinide AUC Produced by ICZ and GEM. The inhibition ratios of repaglinide intrinsic clearances as well as the fm_{2C8} were estimated by regression analysis of the AUC increase by ICZ and GEM using Eqs. 4–10. The R3A4, R2C8, R_{inf}, and fm_{2C8} were optimized at 0.22, 0.045, 0.50, and 0.85, respectively, showing that the reported AUC increase for each condition (control, +ICZ, +GEM, and +ICZ+GEM) can be explained by the CYP3A4, CYP2C8, and OATP1B1 all being inhibited by coadministration of ICZ and GEM. The estimated fm_{2C8} value was used as its initial value in the final fitting analysis of the repaglinide concentration profiles.

Analysis of the ICZ Concentration Profile. The blood concentration profile of ICZ was fitted to Eq. 11 based on the simple PBPK model (Fig. 1A) and the values of $k_{a,icz}$, $V_{b,icz}$, and $CL_{int,icz}$ were optimized to best fit the observed concentration profile. All the parameters for ICZ used in the analyses are summarized in Table 1 together with the estimated values. As shown in Fig. 2A, the obtained concentration profile of ICZ after 3 days of repeated administration was close to the observed values (Jaakkola et al., 2005).

Analysis of the GEM and GEM-glu Concentration Profiles. The blood concentration profiles of GEM and GEM-glu were fitted to Eqs. 16 and 19, respectively, based on the simple PBPK model (Fig. 1B) and the values of $k_{a,gem}$, $V_{b,gem}$, $PS_{eff,gem}$, $PS_{eff,glu}$, CL_{int1}, and $CL_{int,h,glu}$ were optimized to best fit the observed concentration profiles. All parameters used in the analysis are summarized in Table 1 together with the estimated values. As shown in Fig. 2B, the obtained concentration profiles of GEM and GEM-glu after 3 days of repeated administration of GEM were close to the observed values (Tornio et al., 2008).

Analysis of the Repaglinide Concentration Profiles Considering the Interaction with ICZ/GEM. The blood concentration profiles of repaglinide for the four conditions (control, +ICZ, +GEM, and +ICZ +GEM) were analyzed based on the simple PBPK model (Fig. 1C) and differential equations (Eqs. 22–26) together with the concentration profiles of ICZ, GEM, and GEM-glu (Eqs. 11, 12, 16–21). The values of $k_{a,s}$, $V_{b,s}$, $k_{12,s}$, $k_{21,s}$, Lag_s, fm_{2C8}, $K_{i,3A4,icz}$, and $K_{i,1B1,gem}$ were optimized by simultaneous fitting analysis fixing all the parameters for the inhibitors (ICZ, GEM, and GEM-glu) at values shown in Table 1. All the parameters for repaglinide used in the analyses are summarized in Table 2 together with the estimated values. The obtained concentration profiles of repaglinide were close to the observed values for each of the four conditions as shown in Fig. 2C. The repaglinide AUC ratios for +ICZ, +GEM, and +ICZ+GEM conditions were calculated to be 1.2-, 6.5-, 24.3-fold, respectively.

Simulation of the Repaglinide Concentration Profiles in Other Interaction Studies with GEM. The repaglinide concentration increase produced by GEM reported in other interaction studies (Backman et al., 2009; Honkalammi et al., 2011, 2012) were simulated based on the same PBPK model (Figs. 1, B and C; Eqs. 16–26) together with the parameters estimated in the present study (Table 2). Figure 3 shows the observed (Backman et al., 2009) and simulated concentration profiles of repaglinide administered at various intervals after repeated GEM dosing. The persistent interaction, which recovers after 96 hours, was well reproduced in our simulation analysis. Furthermore, the estimated AUC increase agreed well with the observed values for all the conditions investigated (Table 3).

Discussion

The AUC of repaglinide has been reported to be increased 1.4-, 8.1-, or 19.4-fold when healthy volunteers received repaglinide after 3 days of treatment with ICZ, GEM, or both GEM and ICZ, respectively

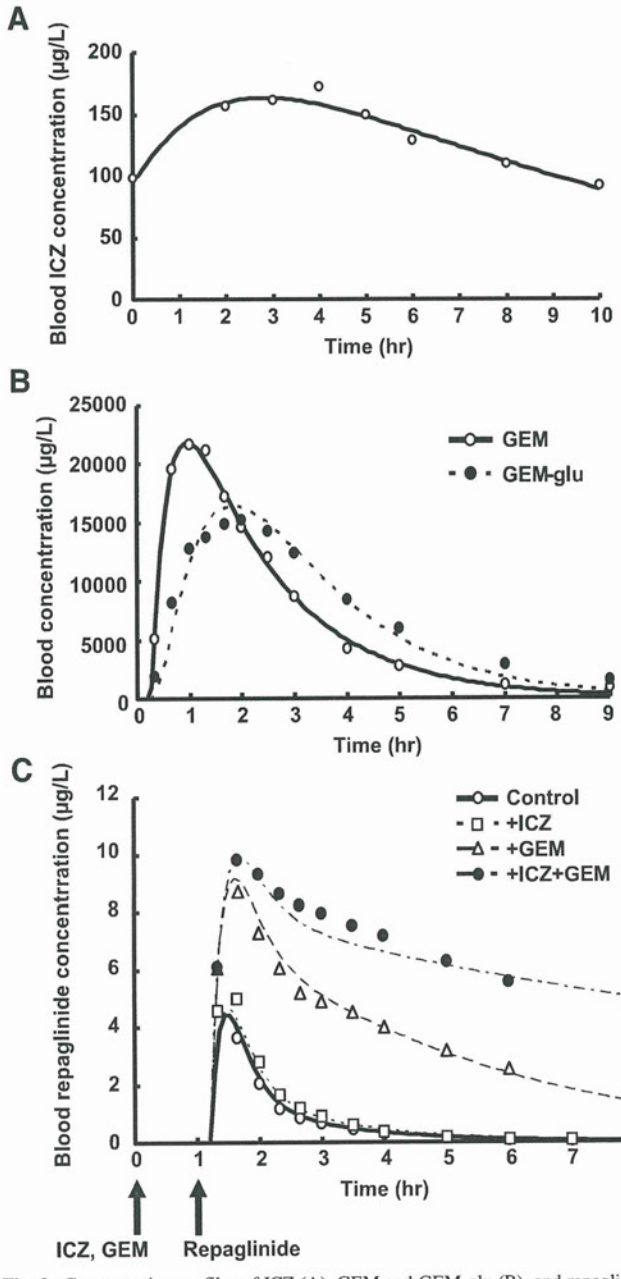

Fig. 2. Concentration profiles of ICZ (A), GEM and GEM-glu (B), and repaglinide (C) in blood. (A) On the basis of the PBPK model (Fig. 1A) and differential equations (Eqs. 11, 12), the time course of the ICZ concentration in blood ($C_{b,icz}$) after 3 days of repeated administration (100 mg p.o., twice a day) was reproduced using the pharmacokinetic (PK) parameters shown in Table 1. The solid line and the open circles indicate the simulated time course and the observed values (Jaakkola et al., 2005), respectively. (B) On the basis of the PBPK model (Fig. 1B) and differential equations (Eqs. 16–21), the time courses of the GEM and GEM-glu concentration in blood ($C_{b,gem}$ and $C_{b,glu}$, respectively) after 3 days of repeated administration of GEM (600 mg p.o., twice a day) were reproduced using the PK parameters shown in Table 1. The solid line and the open circles indicate the simulated time course and the observed values (Tornio et al., 2008), respectively, for GEM; the dotted line and the closed circles indicate the simulated time course and the observed values (Tornio et al., 2008), respectively, for GEM-glu. (C) On the basis of the PBPK model (Fig. 1C) and differential equations (Eqs. 22–26), the time courses of the repaglinide concentration in blood ($C_{b,s}$) for the four conditions (control, +ICZ, +GEM and +ICZ+GEM) were reproduced using the parameters shown in Table 2. The concentration profiles for ICZ and GEM/GEM-glu were simultaneously analyzed using Eqs. 11, 12, and 16–21, respectively, to provide the inhibitor concentrations. The solid line and open circles indicate the simulated time course and the observed values, respectively, for the control condition; the dotted line and open squares indicate the simulated time course and the observed values, respectively, for the +ICZ condition; the broken line and open triangles indicate the simulated time course and the observed values, respectively, for the +GEM condition; and the chain line and closed circles indicate the simulated time course and the observed values, respectively, for the +ICZ+GEM condition.

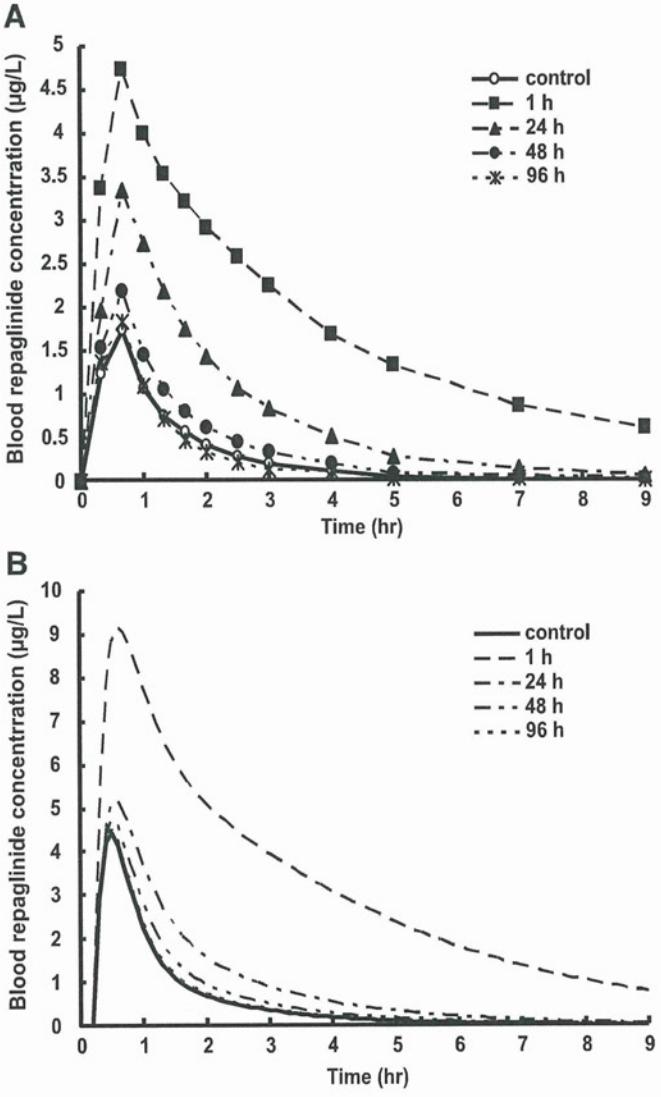

Fig. 3. Observed (A) and simulated (B) concentration profiles of repaglinide in an interaction study with GEM administered at different dosing intervals. (A) Reported repaglinide concentration profiles in healthy volunteers who received a single oral dose of repaglinide (0.25 mg) at different times after GEM (600 mg p.o., twice a day, for 3 days) (Backman et al., 2009). The solid line and open circles represent the profiles for the control condition (without GEM); the broken line and closed squares for the 1-hour interval condition; the chain line and closed triangles for the 24-hour interval condition; the double chain line and closed circles for the 48-hour interval condition; and the dotted line and asterisks for the 96-hour interval condition. (B) Blood concentration profiles of GEM and repaglinide, assuming the same dosing regimen as in (A), were simulated based on the PBPK model shown in Figs. 1, B and C together with the parameters estimated in the present study (Tables 2). The same line as in Fig. 3A was used for each condition.

(Niemi et al., 2003a). The present study investigated whether these interactions can be quantitatively explained by the inhibition of the transporter and enzymes involved in repaglinide disposition on the basis of the clearance concept and simple PBPK modeling.

The major route of repaglinide elimination from the body is hepatic metabolism, with a negligible contribution from renal clearance (f_e = 0.001) (van Heiningen et al., 1999), and the plasma concentration

TABLE 3

Repaglinide AUC increase produced by concomitant GEM administration at various timings/doses

Fold Change in Repaglinide AUC Produced by GEM		
Report 1 (Backman et al., 2009)	Simulated	Reported
Dosing interval between GEM and repaglinide		
1 h	6.49	7.56
24 h	1.78	2.86
48 h	1.25	1.42
96 h	1.05	0.98
Report 2 (Honkalammi et al., 2011)	Simulated	Reported
Dosing interval between GEM and repaglinide		
0 h	4.85	4.98
1 h	6.49	6.36
3 h	5.22	6.59
6 h	3.93	5.43
Report 3 (Honkalammi et al., 2012)	Simulated	Reported
Dose of GEM		
30 mg	3.35	3.40
100 mg	4.22	5.57
600 mg	6.49	7.04

profile of repaglinide has been shown to be affected by the genetic polymorphism of OATP1B1 (Niemi et al., 2005; Kalliokoski et al., 2008) or CYP2C8 (Niemi et al., 2003b, 2005). In the present analysis, therefore, it was assumed that repaglinide is eliminated only from the liver and that both hepatic uptake and metabolism contribute to its hepatic elimination. As a result, the β value in Eq. 2 was calculated to be 0.27 using the optimized values of PS_{eff} and CL_{int} (Table 2), which indicates that its hepatic elimination is not completely limited by the hepatic uptake.

It has been reported that about 66% of orally administered [^{14}C] repaglinide is excreted as a metabolite M2 in the feces and urine in healthy volunteers (van Heiningen et al., 1999). In in vitro studies, M0-OH, M1, M2, M4, and M5 have been reported as metabolites of repaglinide (Bidstrup et al., 2003). At a relatively high concentration of repaglinide (22 μM), formation of M1 by CYP3A4 and M4 by CYP2C8 were the major metabolic pathways in human liver microsomes (Bidstrup et al., 2003). Kajosaari et al. (2005a) investigated the contributions of CYP3A4 and CYP2C8 to the metabolism of repaglinide at a therapeutic repaglinide concentration (< 0.4 μM) using recombinant enzymes, but the results were highly dependent on the scaling factor used. It has also been reported recently that the fm_{2C8} value was estimated to be 0.49, 0.41, and 0.63 in an in vitro study using human hepatocytes, S9 fractions, and liver microsomes, respectively (Säll et al., 2012). In the present study, the estimated fm_{2C8} value of 0.801 (Table 2) indicates a larger contribution of CYP2C8 than CYP3A4, which is consistent with the previous findings that the AUC of repaglinide was affected by the genetic polymorphism of CYP2C8 (Niemi et al., 2003b, 2005) but not CYP3A4 (Ruzilawati and Gan, 2010).

In vitro studies have demonstrated that both GEM and GEM-glu inhibit OATP1B1 (Shitara et al., 2004; Nakagomi-Hagihara et al., 2007; Hinton et al., 2008). The K_i or IC_{50} values for GEM and of GEM-glu were reported to be 72.4 and 24.3 μM, respectively, in OATP1B1-expressing Madin-Darby canine kidney cells (Shitara et al., 2004); 35.8 μM and 9.3 μM, respectively, in human hepatocytes (Nakagomi-Hagihara et al., 2007); and 15.5 and 7.9 μM, respectively,

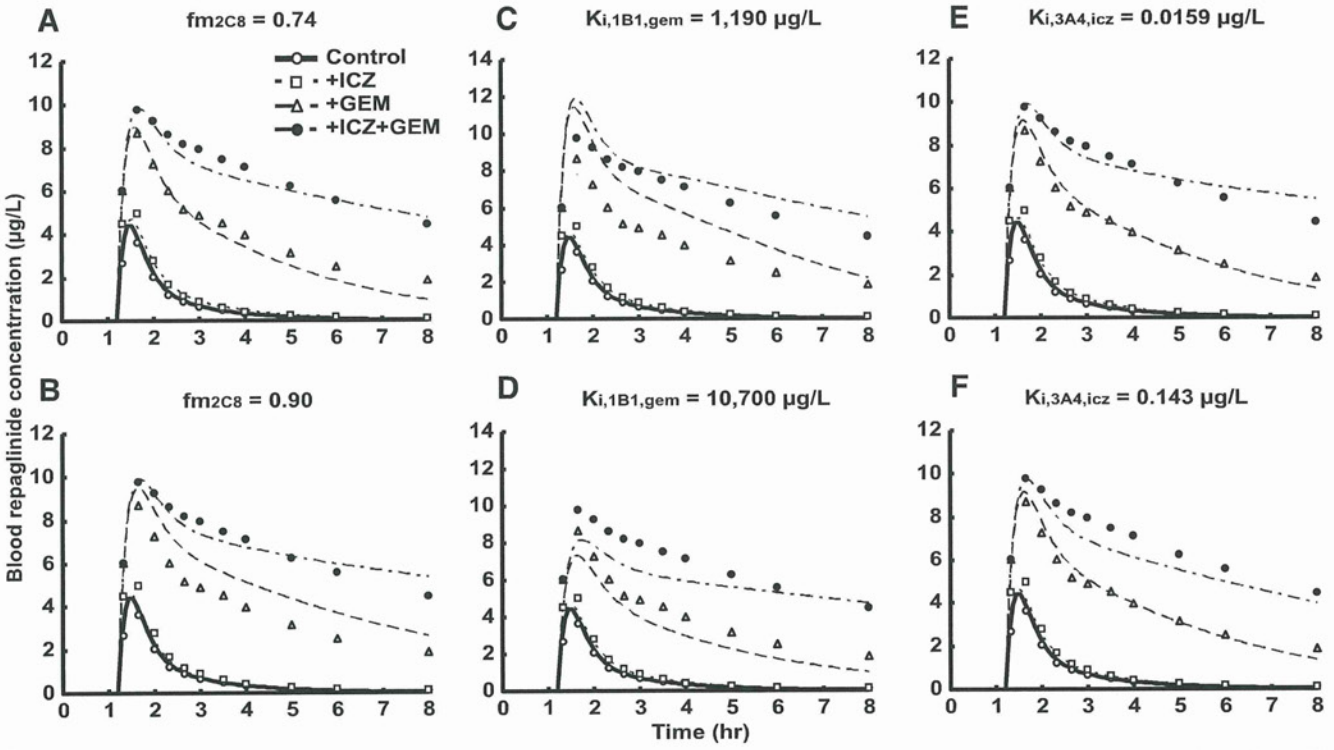

Fig. 4. Sensitivity analysis of the parameters obtained in this study. The concentration profiles of repaglinide were simulated using different values for fm_{2C8} (A and B), $K_{i,1B1,gem}$ (C and D), or $K_{i,3A4,icz}$ (E and F), with other parameters fixed at the same values as in Fig. 2C (the original values for fm_{2C8}, $K_{i,1B1,gem}$, and $K_{i,3A4,icz}$ were 0.801, 3,560 μg/l, and 0.0477 μg/l, respectively). The symbols and lines are same as in Fig. 2C.

in OATP1B1-expressing *Xenopus* oocytes (Nakagomi-Hagihara et al., 2007). In the present fitting analysis, the ratio of $K_{i,1B1glu}$ to $K_{i,1B1gem}$ was fixed at 0.385, the mean ratio calculated from these reported values (0.26–0.51), to reduce the number of unknown parameters. As a result, the estimated K_i values ($K_{i,1B1gem}$ = 14.2±10.1 μM, $K_{i,1B1glu}$ = 5.48 μM) (Table 2) were close to the reported values described above.

Although both GEM and GEM-glu have been also reported to inhibit CYP2C8, the IC_{50} value for GEM was sevenfold higher than that for GEM-glu (Shitara et al., 2004), which was shown to be a mechanism-based inhibitor of CYP2C8 (Ogilvie et al., 2006). In the present study, therefore, only the mechanism-based inhibition of CYP2C8 by GEM-glu was incorporated in the model fixing the $k_{inact,2C8}$ and $K_{i,app,2C8}$ at the reported values (12.6 h^{-1} and 52 μM, respectively) (Ogilvie et al., 2006).

On the basis of a PBPK analysis of reported in vivo interactions between ICZ and CYP3A4 substrates, Kato et al. (2008) reported an in vivo K_i value of 0.282 μg/l (0.4 nM) for ICZ against CYP3A4, which is nearly 500-fold lower than the average K_i value obtained in in vitro studies using human liver microsomes. The $K_{i,3A4,icz}$ value of 0.0477 ± 0.0365 μg/l (0.0676 ± 0.0518 nM) estimated by the present fitting analysis (Table 2) was even smaller than the reported in vivo K_i value, although the contribution of CYP3A4 inhibition to the overall change in repaglinide pharmacokinetics should not be large in the present analysis based on the fm_{2C8} value of 0.801 and the hepatic disposition limited in part by the uptake (β = 0.27).

To confirm the validity of the parameter values obtained in the present study, sensitivity analyses were carried out for fm_{2C8}, $K_{i,1B1,gem}$, and $K_{i,3A4,icz}$. As shown in Fig. 4, the simulated concentration profiles of repaglinide deviated greatly from the observed concentrations when altered values of fm_{2C8} and K_i were used, suggesting the reliability of these parameters estimated in the present analysis. Furthermore, the repaglinide concentration increase by concomitant GEM administration at various timings/doses, reported in other papers, were well reproduced using the same PBPK model together with the parameters estimated in the present study (Fig. 3; Table 3). These results indicate the validity of the PBPK model used in the present analyses as well as the estimated parameters.

In conclusion, the plasma concentration profiles of repaglinide in the interaction study were reproduced by the PBPK model, suggesting that the reported concentration increase by ICZ and GEM results from the inhibition of OATP1B1-mediated hepatic uptake by GEM and GEM-glu and that of CYP2C8- and CYP3A4-mediated metabolism by GEM-glu and ICZ, respectively. The present PBPK model is expected to be applicable to the analyses of other interactions involving both hepatic uptake transporters and metabolic enzymes.

Authorship Contributions

Participated in research design: Kudo, Sugiyama, Ito.

Conducted experiments: Kudo, Ito.

Contributed new reagents or analytic tools: Hisaka.

Performed data analysis: Kudo, Hisaka, Sugiyama, Ito.

Wrote or contributed to the writing of the manuscript: Kudo, Hisaka, Sugiyama, Ito.

References

Backman JT, Kivistö KT, Olkkola KT, and Neuvonen PJ (1998) The area under the plasma concentration-time curve for oral midazolam is 400-fold larger during treatment with itraconazole than with rifampicin. *Eur J Clin Pharmacol* **54**:53–58.

Backman JT, Kyrklund C, Neuvonen M, and Neuvonen PJ (2002) Gemfibrozil greatly increases plasma concentrations of cerivastatin. *Clin Pharmacol Ther* **72**:685–691.

Backman JT, Honkalammi J, Neuvonen M, Kurkinen KJ, Tornio A, Niemi M, and Neuvonen PJ (2009) CYP2C8 activity recovers within 96 hours after gemfibrozil dosing: estimation of CYP2C8 half-life using repaglinide as an in vivo probe. *Drug Metab Dispos* **37**:2359–2366.

Bidstrup TB, Bjørnsdottir I, Sidelmann UG, Thomsen MS, and Hansen KT (2003) CYP2C8 and CYP3A4 are the principal enzymes involved in the human in vitro biotransformation of the insulin secretagogue repaglinide. *Br J Clin Pharmacol* **56**:305–314.

Bidstrup TB, Stilling N, Damkier P, Scharling B, Thomsen MS, and Brøsen K (2004) Rifampicin seems to act as both an inducer and an inhibitor of the metabolism of repaglinide. *Eur J Clin Pharmacol* **60**:109–114.

Davies B and Morris T (1993) Physiological parameters in laboratory animals and humans. *Pharm Res* **10**:1093–1095.

Fuhlendorff J, Rorsman P, Kofod H, Brand CL, Rolin B, MacKay P, Shymko R, and Carr RD (1998) Stimulation of insulin release by repaglinide and glibenclamide involves both common and distinct processes. *Diabetes* **47**:345–351.

Galetin A, Ito K, Hallifax D, and Houston JB (2005) CYP3A4 substrate selection and substitution in the prediction of potential drug-drug interactions. *J Pharmacol Exp Ther* **314**:180–190.

Hatorp V (2002) Clinical pharmacokinetics and pharmacodynamics of repaglinide. *Clin Pharmacokinet* **41**:471–483.

Hinton LK, Galetin A, and Houston JB (2008) Multiple inhibition mechanisms and prediction of drug-drug interactions: status of metabolism and transporter models as exemplified by gemfibrozil-drug interactions. *Pharm Res* **25**:1063–1074.

Hisaka A and Sugiyama Y (1998) Analysis of nonlinear and nonsteady state hepatic extraction with the dispersion model using the finite difference method. *J Pharmacokinet Biopharm* **26**:495–519.

Honkalammi J, Niemi M, Neuvonen PJ, and Backman JT (2011) Mechanism-based inactivation of CYP2C8 by gemfibrozil occurs rapidly in humans. *Clin Pharmacol Ther* **89**:579–586.

Honkalammi J, Niemi M, Neuvonen PJ, and Backman JT (2012) Gemfibrozil is a strong inactivator of CYP2C8 in very small multiple doses. *Clin Pharmacol Ther* **91**:846–855.

Ito K, Ogihara K, Kanamitsu S, and Itoh T (2003) Prediction of the in vivo interaction between midazolam and macrolides based on in vitro studies using human liver microsomes. *Drug Metab Dispos* **31**:945–954.

Jaakkola T, Backman JT, Neuvonen M, and Neuvonen PJ (2005) Effects of gemfibrozil, itraconazole, and their combination on the pharmacokinetics of pioglitazone. *Clin Pharmacol Ther* **77**:404–414.

Jones HM, Barton HA, Lai Y, Bi YA, Kimoto E, Kempshall S, Tate SC, El-Kattan A, Houston JB, and Galetin A, et al. (2012) Mechanistic pharmacokinetic modeling for the prediction of transporter-mediated disposition in humans from sandwich culture human hepatocyte data. *Drug Metab Dispos* **40**:1007–1017.

Kajosaari LI, Laitila J, Neuvonen PJ, and Backman JT (2005a) Metabolism of repaglinide by CYP2C8 and CYP3A4 in vitro: effect of fibrates and rifampicin. *Basic Clin Pharmacol Toxicol* **97**:249–256.

Kajosaari LI, Niemi M, Backman JT, and Neuvonen PJ (2006) Telithromycin, but not montelukast, increases the plasma concentrations and effects of the cytochrome P450 3A4 and 2C8 substrate repaglinide. *Clin Pharmacol Ther* **79**:231–242.

Kajosaari LI, Niemi M, Neuvonen M, Laitila J, Neuvonen PJ, and Backman JT (2005b) Cyclosporine markedly raises the plasma concentrations of repaglinide. *Clin Pharmacol Ther* **78**:388–399.

Kalliokoski A, Backman JT, Kurkinen KJ, Neuvonen PJ, and Niemi M (2008) Effects of gemfibrozil and atorvastatin on the pharmacokinetics of repaglinide in relation to SLCO1B1 polymorphism. *Clin Pharmacol Ther* **84**:488–496.

Kanamitsu S, Ito K, and Sugiyama Y (2000) Quantitative prediction of in vivo drug-drug interactions from in vitro data based on physiological pharmacokinetics: use of maximum unbound concentration of inhibitor at the inlet to the liver. *Pharm Res* **17**:336–343.

Kato M, Shitara Y, Sato H, Yoshisue K, Hirano M, Ikeda T, and Sugiyama Y (2008) The quantitative prediction of CYP-mediated drug interaction by physiologically based pharmacokinetic modeling. *Pharm Res* **25**:1891–1901.

Kilford PJ, Stringer R, Sohal B, Houston JB, and Galetin A (2009) Prediction of drug clearance by glucuronidation from in vitro data: use of combined cytochrome P450 and UDP-glucuronosyltransferase cofactors in alamethicin-activated human liver microsomes. *Drug Metab Dispos* **37**:82–89.

Kyrklund C, Backman JT, Neuvonen M, and Neuvonen PJ (2003) Gemfibrozil increases plasma pravastatin concentrations and reduces pravastatin renal clearance. *Clin Pharmacol Ther* **73**:538–544.

Ménochet K, Kenworthy KE, Houston JB, and Galetin A (2012) Use of mechanistic modeling to assess interindividual variability and interspecies differences in active uptake in human and rat hepatocytes. *Drug Metab Dispos* **40**:1744–1756.

Nakagomi-Hagihara R, Nakai D, Tokui T, Abe T, and Ikeda T (2007) Gemfibrozil and its glucuronide inhibit the hepatic uptake of pravastatin mediated by OATP1B1. *Xenobiotica* **37**:474–486.

Niemi M, Backman JT, Kajosaari LI, Leathart JB, Neuvonen M, Daly AK, Eichelbaum M, Kivistö KT, and Neuvonen PJ (2005) Polymorphic organic anion transporting polypeptide 1B1 is a major determinant of repaglinide pharmacokinetics. *Clin Pharmacol Ther* **77**:468–478.

Niemi M, Backman JT, Neuvonen M, and Neuvonen PJ (2003a) Effects of gemfibrozil, itraconazole, and their combination on the pharmacokinetics and pharmacodynamics of repaglinide: potentially hazardous interaction between gemfibrozil and repaglinide. *Diabetologia* **46**:347–351.

Niemi M, Backman JT, Neuvonen M, Neuvonen PJ, and Kivistö KT (2000) Rifampin decreases the plasma concentrations and effects of repaglinide. *Clin Pharmacol Ther* **68**:495–500.

Niemi M, Leathart JB, Neuvonen M, Backman JT, Daly AK, and Neuvonen PJ (2003b) Polymorphism in CYP2C8 is associated with reduced plasma concentrations of repaglinide. *Clin Pharmacol Ther* **74**:380–387.

Niemi M, Kajosaari LI, Neuvonen M, Backman JT, and Neuvonen PJ (2004) The CYP2C8 inhibitor trimethoprim increases the plasma concentrations of repaglinide in healthy subjects. *Br J Clin Pharmacol* **57**:441–447.

Niemi M, Neuvonen PJ, and Kivistö KT (2001) The cytochrome P4503A4 inhibitor clarithromycin increases the plasma concentrations and effects of repaglinide. *Clin Pharmacol Ther* **70**:58–65.

Ogilvie BW, Zhang D, Li W, Rodrigues AD, Gipson AE, Holsapple J, Toren P, and Parkinson A (2006) Glucuronidation converts gemfibrozil to a potent, metabolism-dependent inhibitor of CYP2C8: implications for drug-drug interactions. *Drug Metab Dispos* **34**:191–197.

Poulin P and Theil FP (2002) Prediction of pharmacokinetics prior to in vivo studies. II. Generic physiologically based pharmacokinetic models of drug disposition. *J Pharm Sci* **91**:1358–1370.

Rowland Yeo K, Jamei M, Yang J, Tucker GT, and Rostami-Hodjegan A (2010) Physiologically based mechanistic modelling to predict complex drug-drug interactions involving simultaneous competitive and time-dependent enzyme inhibition by parent compound and its metabolite in both liver and gut - the effect of diltiazem on the time-course of exposure to triazolam. *Eur J Pharm Sci* **39**:298–309.

Ruzilawati AB and Gan SH (2010) CYP3A4 genetic polymorphism influences repaglinide's pharmacokinetics. *Pharmacology* **85**:357–364.

Säll C, Houston JB, and Galetin A (2012) A comprehensive assessment of repaglinide metabolic pathways: impact of choice of in vitro system and relative enzyme contribution to in vitro clearance. *Drug Metab Dispos* **40**:1279–1289.

Schneck DW, Birmingham BK, Zalikowski JA, Mitchell PD, Wang Y, Martin PD, Lasseter KC, Brown CD, Windass AS, and Raza A (2004) The effect of gemfibrozil on the pharmacokinetics of rosuvastatin. *Clin Pharmacol Ther* **75**:455–463.

Shitara Y, Hirano M, Sato H, and Sugiyama Y (2004) Gemfibrozil and its glucuronide inhibit the organic anion transporting polypeptide 2 (OATP2/OATP1B1:SLC21A6)-mediated hepatic uptake and CYP2C8-mediated metabolism of cerivastatin: analysis of the mechanism of the clinically relevant drug-drug interaction between cerivastatin and gemfibrozil. *J Pharmacol Exp Ther* **311**:228–236.

Shitara Y, Horie T, and Sugiyama Y (2006) Transporters as a determinant of drug clearance and tissue distribution. *Eur J Pharm Sci* **27**:425–446.

Thummel KE, Shen DD, and Isoherranen N (2011) Appendix II. Design and optimization of dosage regimens: pharmacokinetic data, in *Goodman & Gilman's The Pharmacological Basis of Therapeutics*, 12th ed (Brunton LL, Chabner BA, and Knollmann BC, eds, McGraw-Hill, New York.

Tornio A, Niemi M, Neuvonen M, Laitila J, Kalliokoski A, Neuvonen PJ, and Backman JT (2008) The effect of gemfibrozil on repaglinide pharmacokinetics persists for at least 12 h after the dose: evidence for mechanism-based inhibition of CYP2C8 in vivo. *Clin Pharmacol Ther* **84**:403–411.

van Heiningen PN, Hatorp V, Kramer Nielsen K, Hansen KT, van Lier JJ, De Merbel NC, Oosterhuis B, and Jonkman JH (1999) Absorption, metabolism and excretion of a single oral dose of (14)C-repaglinide during repaglinide multiple dosing. *Eur J Clin Pharmacol* **55**:521–525.

Varhe A, Olkkola KT, and Neuvonen PJ (1994) Oral triazolam is potentially hazardous to patients receiving systemic antimycotics ketoconazole or itraconazole. *Clin Pharmacol Ther* **56**:601–607.

von Moltke LL, Greenblatt DJ, Schmider J, Duan SX, Wright CE, Harmatz JS, and Shader RI (1996) Midazolam hydroxylation by human liver microsomes in vitro: inhibition by fluoxetine, norfluoxetine, and by azole antifungal agents. *J Clin Pharmacol* **36**:783–791.

Wang JS, Neuvonen M, Wen X, Backman JT, and Neuvonen PJ (2002) Gemfibrozil inhibits CYP2C8-mediated cerivastatin metabolism in human liver microsomes. *Drug Metab Dispos* **30**:1352–1356.

Watanabe T, Kusuhara H, Maeda K, Shitara Y, and Sugiyama Y (2009) Physiologically based pharmacokinetic modeling to predict transporter-mediated clearance and distribution of pravastatin in humans. *J Pharmacol Exp Ther* **328**:652–662.

Yabe Y, Galetin A, and Houston JB (2011) Kinetic characterization of rat hepatic uptake of 16 actively transported drugs. *Drug Metab Dispos* **39**:1808–1814.

Yang J, Liao M, Shou M, Jamei M, Yeo KR, Tucker GT, and Rostami-Hodjegan A (2008) Cytochrome p450 turnover: regulation of synthesis and degradation, methods for determining rates, and implications for the prediction of drug interactions. *Curr Drug Metab* **9**:384–394.

Yoshida K, Maeda K, and Sugiyama Y (2012) Transporter-mediated drug—drug interactions involving OATP substrates: predictions based on in vitro inhibition studies. *Clin Pharmacol Ther* **91**:1053–1064.

Zhang X, Quinney SK, Gorski JC, Jones DR, and Hall SD (2009) Semiphysiologically based pharmacokinetic models for the inhibition of midazolam clearance by diltiazem and its major metabolite. *Drug Metab Dispos* **37**:1587–1597.

Zhao P, Vieira Mde L, Grillo JA, Song P, Wu TC, Zheng JH, Arya V, Berglund EG, Atkinson AJ, Jr , and Sugiyama Y, et al. (2012) Evaluation of exposure change of nonrenally eliminated drugs in patients with chronic kidney disease using physiologically based pharmacokinetic modeling and simulation. *J Clin Pharmacol* **52**(1, Suppl)91S–108S.

Address correspondence to: Dr. Kiyomi Ito, Musashino University, Research Institute of Pharmaceutical Sciences, 1-1-20 Shinmachi, Nishitokyo-shi, Tokyo 202-8585, Japan. E-mail: k-ito@musashino-u.ac.jp

DMD DRUG METABOLISM AND DISPOSITION aspet

Journal of
Clinical Pharmacy and Therapeutics

Journal of Clinical Pharmacy and Therapeutics, 2013 doi: 10.1111/jcpt.12063

Development of a detection algorithm for statin-induced myopathy using electronic medical records

K. Sai* PhD, T. Hanatani*† MSc, Y. Azuma* MSc, K. Segawa* PhD, M. Tohkin*† PhD, H. Omatsu‡ PhD, H. Makimoto‡ MSc, M. Hirai‡ PhD and Y. Saito* PhD

**Division of Medicinal Safety Science, National Institute of Health Sciences, Tokyo, †Department of Regulatory Science, Graduate School of Pharmaceutical Sciences, Nagoya City University, Nagoya, and ‡Department of Hospital Pharmacy, Kobe University Hospital, Kobe, Japan*

Received 27 February 2013, Accepted 7 March 2013

Keywords: **detection algorithm, electronic medical records, myopathy, pharmacovigilance, rhabdomyolysis, statin**

SUMMARY

What is known and Objectives: **Demonstration of the utility of electronic medical records (EMRs) for pharmacovigilance (PV) has been highly anticipated. Analysis using appropriately selected EMRs should enable accurate estimation of adverse drug event (ADE) frequencies and thus promote appropriate regulatory actions. Statin-induced myopathy (SIM) is a clinically important ADE, but pharmacoepidemiological methodology for detecting this ADE with high predictability has not yet been established. This study aimed to develop a detection algorithm, highly selective for SIM using EMRs.**

Methods: **We collected EMRs on prescriptions, laboratory tests, diagnoses and medical practices from the hospital information system of Kobe University Hospital, Japan, for a total of 5109 patients who received a statin prescription from April 2006 to March 2009. The current algorithm for extracting SIM-suspected patients consisted of three steps: (i) event detection: increase in creatine kinase (CK) and subsequent statin discontinuation, (ii) filtration by exclusion factors (disease diagnosis/medical practices) and (iii) refinement by the time course of CK values (baseline, event and recovery). A causal relationship between the event and statin prescription (probable/possible/unlikely) was judged by review of patient medical charts by experienced pharmacists. The utility of the current algorithm was assessed by calculating the positive predictive value (PPV). In a comparative analysis, subjects screened in step 1 were extracted by the diagnostic term/code for 'myopathy/rhabdomyolysis', and the PPV of this diagnostic data approach was also estimated.**

Results and Discussion: **Five subjects with suspected SIM were identified using our proposed algorithm, giving a frequency of 0·1% for the adverse event. Review of the medical charts revealed that the causal association of SIM with statin use was judged as 'Likely (probable/possible)' for all five suspected patients; thus, the PPV was estimated as 100% (95% confidence interval: 56·6–100%). The higher utility of the current algorithm compared with the diagnostic data approach was also shown by assessing the PPV (100 vs. 33·3%).**

What is new and Conclusion: **We report on a detection algorithm with high predictability for SIM using EMRs. Combined use of exclusion criteria for disease, medical practice data and time course of CK values contributes to better prediction of SIM. The utility of the proposed algorithm should be further confirmed in a larger study.**

Correspondence: K. Sai, Division of Medicinal Safety Science, National Institute of Health Sciences, Kamiyoga 1-18-1, Setagaya-ku, Tokyo 158-8501, Japan. Tel.: +81 3 3700 1226; fax: +81 3 3700 9788; e-mail: sai@nihs.go.jp

WHAT IS KNOWN AND OBJECTIVES

Pharmacovigilance (PV) is very important for ensuring medicinal drug safety, and currently, a spontaneous reporting system for adverse drug events (ADEs) is the major tool for PV in many countries, including Japan. Recently, the value of electronic medical records (EMRs) captured in hospital information systems (HIS) has been the focus of considerable research because analysis using appropriately selected EMRs may provide accurate estimation of ADE frequencies and hence facilitate appropriate regulatory actions.[1–9] Much effort has been directed at standardizing medical information in EMRs or insurance claims data to promote active PV surveillance in several countries.[10–14] In the United States, the FDA has developed the Sentinel Initiative and has already amassed a healthcare database of 100 million patients.[10,11] In Japan, a medical information database based on a standardized HIS with 10 million patients is planned for 2015. To utilize EMRs for effective PV actions, it is particularly important to develop and validate scientific methodologies for ADE detection that would be applicable to routine surveillance.

Myopathy is a clinically important ADE, caused by a variety of medicinal drugs, especially the lipid-lowering statins.[15–19] It is a clinical syndrome associated with the breakdown of skeletal muscle, accompanied with myalgia and muscular weakness. Although there is no global consensus on criteria for myopathy, it is generally classified, in terms of increasing severity, as myalgia, myositis and rhabdomyolysis. Myositis and rhabdomyolysis are detected clinically by an increase in serum creatine kinase (CK). Rhabdomyolysis, the most severe form, is often accompanied by severe acute renal failure, due to the release of a large amount of myoglobin from damaged muscles into the bloodstream, and occasionally leads to death or requires long-lasting renal dialysis.[20] Because of this, rhabdomyolysis is a high-priority ADE in active PV surveillance worldwide.[21] According to reports in the United States, 0·1–0·2% of patients treated with statins experienced myopathy,[15–18] and the incidence of serious rhabdomyolysis requiring hospitalization was reported to be 0·44 [95% confidence interval (CI), 0·20–0·84]/10 000 person-years for monotherapy with atorvastatin, pravastatin or simvastatin; the incidence increased to 5·98 (95% CI, 0·72–216·0)/10 000 person-years when statin therapy is combined with a fibrate.[19] Considering the likely under-reporting of milder symptoms or with other complications, a much larger number of patients may suffer from myopathy after taking a statin.

Several studies of the detection of drug-related myopathies using EMRs based on diagnostic codes or laboratory tests for CK values have highlighted several issues: for example, high false-positive rates with diagnostic data alone and insufficient discrimination from primary diseases that cause increases in CK values.[13,22,23]

In the current study, we aimed to develop a detection algorithm with high selectivity for statin-induced myopathy (SIM), in terms of myositis and rhabdomyolysis, using EMRs. For this purpose, we combined the data in EMRs for prescriptions, laboratory tests, disease diagnosis and medical practice data and constructed a three-step procedure based on the relationships between statin prescription and the time course of CK values and defined exclusion criteria. We then evaluated the utility of our proposed algorithm by reviewing medical charts of patients screened in the first step.

METHODS

Source of medical information data

We collected the linkable, anonymous EMRs of patients who received a statin from April 2006 to March 2009 from the HIS of Kobe University Hospital, Japan. Data collected from the EMRs included patient background (age, sex, diagnosis and treatment department), prescriptions of statins, laboratory test results including serum CK, diagnostic data [terms with International Classification of Diseases (ICD)-10 codes] and medical practice data on treatments/surgeries (terms with JK codes that are used for claims for medical treatment fees in Japan). Paper-based medical charts from April 2006 to March 2008 and computerized charts from April 2008 to March 2009 were used. Patient demographics are summarized in Table 1. This study was approved by the ethics committees of the National Institute of Health Sciences and Kobe University Hospital.

Development of the detection algorithm

The procedures for extracting and evaluating patients with suspected SIM were as follows (see Figs 1 and 2).

Table 1. Patient demographics

	Number/value
Total patient number	5109
Male/Female	2347/2762
Starting age of statin treatment, years (mean ± SD)	66 ± 12·7
Number of inpatients/outpatients (with overlap)	3143/4433
Total number of departments	39
Patients in major departments	
Cardiovascular internal medicine	1565
Diabetes and endocrinology	1370
Cardiovascular surgery	607
Geriatrics	437
Patients with statin treatment (with overlap)	
Atorvastatin	1979
Pravastatin	1540
Pitavastatin	874
Rosuvastatin	753
Simvastatin	504
Fluvastatin	204

Step 1: event detection. The types of myopathy we targeted were myositis and rhabdomyolysis, which are generally thought to be detectable by an increase in CK values. We defined the criterion (threshold) for SIM as three times the upper limit of the normal (ULN) CK value: 750 IU/L for males and 500 IU/L for females, respectively, were used for this study. Patients with increased CK values, no less than the threshold level and with subsequent statin discontinuation, were identified. The event period was defined as the period during which CK values were no less than the threshold level.

Step 2: filtration by exclusion factors. Cases with non-statin-related CK increases were removed using diagnostic data (terms with ICD-10 codes) and medical practice data (terms with JK codes). Diagnostic terms searched in the current algorithm included acute cardiovascular diseases, primary diseases (brain, muscle and thyroid), serious infection, serious digestive trouble and ascites (Table S1). Medical practice terms included treatments (wound healing care or drainage) and surgeries (craniotomy, thoracotomy, laparotomy, etc.) (Table S2). The time window for disease diagnosis for exclusion was 7 days before/after and throughout the event period, except for hypothyroidism (Fig. 2). For hypothyroidism, the time window after the event period was extended to 30 days, considering a diagnostic process of approximately 1 month. For the medical practices, the window was set as 7 days before and throughout the event period. This study adopted primarily a text search for the terms together with the coding data to obtain more accurate information (Tables S1 and S2).

The diagnostic terms/codes for 'myopathy/rhabdomyolysis' were also captured with the 7-day time window before/after and throughout the event period, but this information was used only as complementary information, and patients were removed when the other exclusion terms/codes were recorded.

Step 3: refinement by the time course of CK values. The time course of CK values throughout the baseline, event and recovery periods was evaluated based on the following criteria: (i) the threshold level for baseline (before the first statin prescription) was defined as the ULN of CK: 250 IU/L for males and 170 IU/L for females, respectively, were used for this study, and the observation period for baseline was within 60 days before the first statin prescription. Accordingly, the patients with CK values at baseline more than the threshold level were removed. (ii) The time period for the event (CK $\geq$ 3x the ULN) was restricted from the day of the last prescription to 15 days after the final day of ingestion (e.g. if a patient was prescribed a statin for 7 days at the last prescription, the time window was 21 days from the last prescription). (iii) The threshold level for recovery was defined as three times the ULN of CK, and the time period for recovery with no recurrence was set as within 60 days from the first day of the event. Accordingly, patients with recovery after the time window (outside of the recovery period) or with recurrence were removed. If CK testing data on baseline and recovery were unavailable within the evaluation window, those subjects were not ruled out in this study.

Evaluation of the algorithm and the diagnostic approach used in reviewing medical charts

The medical charts of the patients extracted in the step 1 (n = 100) were reviewed by two experienced hospital pharmacists with wide medical knowledge. A causal relationship between statin

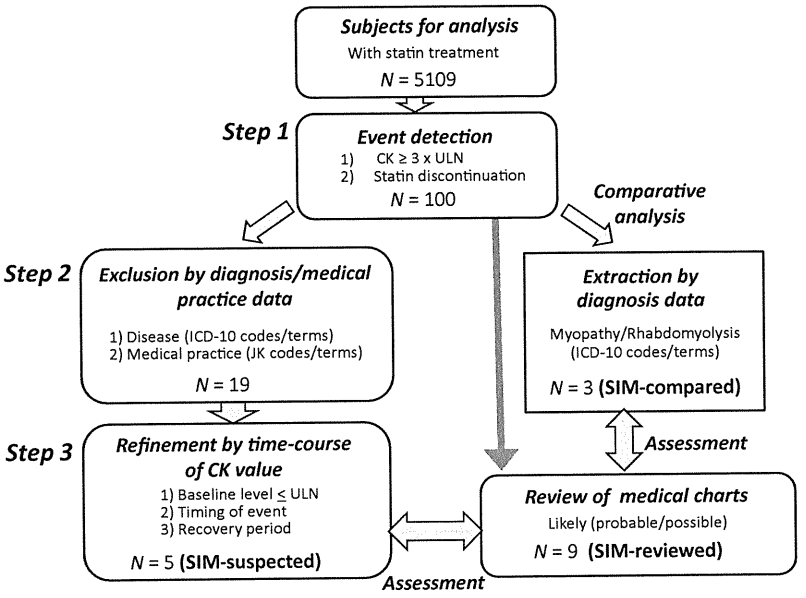

Fig. 1. Scheme and results of algorithm-based extractions of patients suspected to have experienced statin-induced myopathy using electronic medical records and validation by medical chart review. CK, creatine kinase; ULN, upper limit of normal.

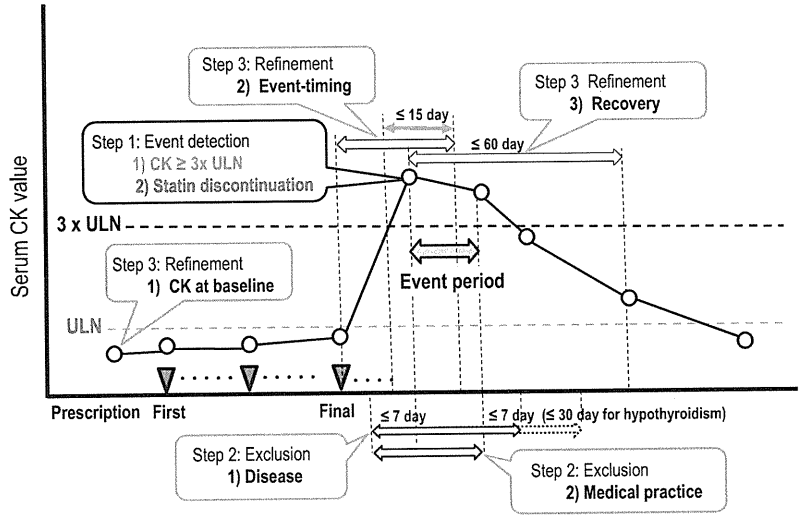

Fig. 2. Diagram of the developed algorithm for detecting statin-induced myopathy. CK, creatine kinase; d, days; ULN, upper limit of normal.

prescription and the event was assessed, and the judgements were classified into three categories: that is, '(A) Probable': with a description for relevance of the statin prescription to the event, '(B) Possible': with no description of any factors that increase CK values and '(C) Unlikely': with a description on non-statin-related causes during the event period (Table 2). The positive predictive value (PPV) for each assessment in the current algorithm against the subjects judged as 'Likely (probable/possible) [(A) plus (B)]' by medical chart review was estimated by Wilson's formula with SAS version 9·3 (SAS Institute Inc., Cary, NC, USA). As a comparative analysis, the subjects screened in step 1 were filtered using a general approach based on the diagnostic term/code for 'myopathy/rhabdomyolysis', and the PPV of this approach was also estimated.

RESULTS

SIM-suspected patients detected using the proposed algorithm

Five thousand one hundred and nine patients, treated with statins, were eligible for inclusion in this study. The patients' demographics are summarized in Table 1. Figure 1 shows the process for extraction and validation of patients with suspected SIM, in terms of myositis and rhabdomyolysis, using EMRs. Of the 5109 patients, 100 subjects who experienced the event were detected (step 1). In the next step, to exclude non-statin-related causes of CK increase using diagnostic and medical practice data (see Methods and Tables S1 and S2), 81 subjects were removed, leaving 19 subjects for step 3. In this final step, consisting of careful examination of the

Table 2. Classification of causal relationships between the event and statin prescription by medical chart review

Category	Criteria
(A) Probable	With description implicating relationship of statin prescription
(B) Possible	With no description of any non-statin-related causes[a]
(C) Unlikely	With description on non-statin-related causes[a]

[a]Major non-statin-related causes for CK increases include surgery, acute cardiovascular disease, primary diseases (brain, muscle and thyroid), serious infection, serious enteritis, ascites and excessive muscular exercise.

Table 3. Judgment on statin-induced myopathy by medical chart review[a]

Category	Description	Number of patients
(A) Probable		3
(B) Possible		6
(C) Unlikely	Surgery	64
	Acute cardiovascular disease	16
	Primary disease	8
	Other[b]	3

[a]For 100 patients screened in step 1.
[b]Includes sepsis, ascites and excessive exercise.

time course of CK values carefully, five subjects were identified as SIM-suspected patients (Table S3). This led to an estimated frequency of SIM-suspected patients of 0·1% (5/5109).

Review of medical charts

To assess the utility of the proposed algorithm, the descriptions in the medical charts for all 100 patients screened in step 1 were manually reviewed by experienced pharmacists, and causal relationships between the event and statin prescription were determined based on the criteria summarized in Table 2. The results were classified into three categories, that is, '(A) Probable', '(B) Possible' and '(C) Unlikely', judging from descriptions on drug relevance and/or the text information on factors that may increase CK values. With the current criteria, three and six subjects were judged as '(A) Probable' and '(B) Possible', respectively, and 91 were classified as '(C) Unlikely'. The major causes for '(C) Unlikely' were surgeries [70% of (C)] and acute cardiovascular diseases (18%), and the other factors included primary diseases and serious symptoms with infection and ascites (Table 3).

By cross-checking the results obtained with the algorithm and the medical charts, of the five subjects detected as SIM-suspected patients with the algorithm, three were judged as '(A) Probable' in the medical charts and two were judged as '(B) Possible'. Four other subjects who were judged as '(B) Possible' by review of the medical charts, because of no description of any non-statin-related causes, were not identified by the algorithm. These four patients were excluded in step 3 of the algorithm because the event timings exceeded the 15-day window after the final day of ingestion for all four patients, and the baseline CK values were over the ULN for three patients.

Assessment of the proposed algorithm

For assessing the predictability of the current algorithm, the PPV was estimated for each step. We considered that the manual review results of both '(A) Probable' and '(B) Possible' were 'Likely' for a causal relationship (Fig. 1), and then, the PPV for 'Likely [(A) plus (B)]' was calculated. The PPVs increased depending on the number of steps, and the PPV for the SIM-suspected patients extracted at the final step was estimated as 100% (95% CI: 56·6–100%) (Table 4).

Comparison for SIM detection using diagnostic data

We compared the predictabilities between the current algorithm and a general approach using diagnostic data, terms/codes 'myopathy/rhabdomyolysis' (Fig. 1). Among the 100 patients screened in step 1, three were found to have received a diagnosis of rhabdomyolysis. By reviewing the medical charts, we found that only one patient among the three was judged as '(A) Probable', and the other two subjects were judged as '(C) Unlikely' because other non-statin-related causes were identified. Accordingly, the PPV for the diagnostic data approach (SIM compared) was 33·3% (95% CI: 61·5–79·2%), which was much lower than that of the proposed algorithm (SIM suspected) (Table 4). The proposed algorithm appropriately identified the one '(A) Probable' patient and removed the two '(C) Unlikely' patients by detecting the non-drug-related disease for the one patient and the higher baseline CK level for the other patient (step 3).

DISCUSSION

Many studies have demonstrated the potential usefulness of monitoring of medical data for discontinuation/switching of prescriptions with newly recorded diagnoses, for early detection of serious ADEs, such as acute cardiovascular events and

Table 4. Results of the algorithm-based method and its assessment by medical chart review

Step in algorithm	Patient number		
	Screened by algorithm	Judged as 'Likely'[a]	PPV (95% confidence interval)
Developed algorithm			
Step 1: event detection by CK increase and statin discontinuation	100	9	9·0% (14·8–16·2%)
Step 2: exclusion by terms/codes	19	9	47·4% (27·3–68·3%)
Step 3: refinement by CK time course (SIM-suspected)	5	5	100% (56·6–100%)
Comparative analysis			
Step 1 and extraction by diagnosis data[b] (SIM-compared)	3	1	33·3% (61·5–79·2%)

[a]Classified into '(A) Probable' or '(B) Possible' by medical chart review.
[b]ICD-10 codes/terms for myopathy/rhabdomyolysis.

rhabdomyolysis.[7–9] These studies suggest that use of diagnostic data is useful when the incidence rate for the target ADE is relatively high[24] and when the ADE is detectable as a definitive endpoint, with well-established diagnostic criteria and a unique code. However, use of diagnostic records alone has several limitations as diagnosis could be variable depending on the physician's judgement, especially if definitive criteria have not been established, as in the case of rhabdomyolysis, and input errors also occur.[25] For complementing this approach, the usefulness of more objective laboratory test data for detecting ADEs has been recognized.[13,22,23,26,27] However, judgements based on abnormal test values also have limitations, because many diseases may cause abnormal test results.[13,22,23] A recent study showed an efficient screening method for rhabdomyolysis by consideration of both abnormal CK test values and diseases that may cause such abnormal values.[23] However, because automated screening was used prior to manual review, a substantial number of false-positive subjects still remained. Therefore, for a more discriminative method for SIM detection using EMRs, additional criteria should be considered.

In the current study, we developed a detection algorithm for SIM, aiming at more selective detection for drug-related events, considering the relationships between statin prescription and time course of CK values and appropriate exclusion criteria. In the exclusion process, we used not only diagnostic data on typical diseases, such as acute cardiac infarction, but also on medical practice data, including the treatments/surgeries, and set up appropriate time windows depending on properties of diseases/medical practice. In this process, we used both the terms and the coding data, because text searches could capture information more accurately than coding data alone. Furthermore, to exclude other causes that may not have been recorded during the observation period but could have affected the CK values, these were assessed at baseline and the timings of event and recovery were also evaluated in the final process.

The PPV revealed that the single step 1 process yielded a high rate of false positives, showing that more than 90% of the events were non-statin-related. Thus, our findings and also those of others[13,22,23] show that detection of abnormal CK values alone is insufficient for predicting SIM. The next exclusion procedure (step 2) identified the affected subjects more precisely but the PPV was still low (47·4%). Refining the process with consideration of the time course of CK values (step 3) led to a PPV of 100% (95% CI: 56·6–100%) for SIM-suspected patients (Table 4). Thus, additional criteria on medical practices and refinement of CK values would appear critical for improving the detection of SIM.

The medical chart review revealed that of the nine subjects judged as 'Likely', five subjects were detected by the algorithm (SIM suspected). The four remaining subjects classified as '(B) Possible' in the medical chart review were removed in step 3 of the algorithm (Fig. 1 and Table 4). We speculate that this discrepancy may be attributable to descriptions in medical charts not always being sufficient for establishing a causal relationship, particularly when a common criterion has not been established, for the event, as exemplified by rhabdomyolysis. The frequency of SIM-suspected patients detected by application of the algorithm was 0·1% and is consistent with previous reports.[15–18]

There are several limitations in our study. Because of the small number of patients from one hospital, selection bias of the source population cannot be excluded and reliable comparison of the incidence of SIM with different statins cannot be made. Therefore, studies of a larger population are needed to confirm the usefulness of the current algorithm.

WHAT IS NEW AND CONCLUSION

We report on a detection algorithm with high predictability for SIM using EMRs. Combined use of exclusion criteria for disease, medical practice data and time course of CK values contributes to better prediction of SIM. The utility of the proposed algorithm should be further confirmed in a larger study.

ACKNOWLEDGEMENTS

This study was supported in part by the Health and Labour Sciences Research grant from the Ministry of Health, Labour and Welfare in Japan.

CONFLICT OF INTEREST

YS received a Health and Labour Sciences Research grant from the Ministry of Health, Labour and Welfare in Japan. The other authors declare no conflict of interest.

SUPPORTING INFORMATION

Additional Supporting Information may be found in the online version of this article:

Table S1. Terms of diseases and corresponding ICD-10 codes for searches in the current algorithm (step 2)

Table S2. Terms of medical practices for searches in the current algorithm (step 2)

Table S3. Profile of patients suspected to have experienced statin-induced myopathy

REFERENCES

1. Wise L, Parkinson J, Raine J, Breckenridge A. New approaches to drug safety: a pharmacovigilance tool kit. *Nat Rev Drug Discov*, 2009;**8**:779–782.
2. Lu Z. Information technology in pharmacovigilance: benefits, challenges, and future directions from industry perspectives. *Drug Healthc Patient Saf*, 2009;**1**:35–45.
3. Harpaz R, Vilar S, Dumouchel W *et al.* Combing signals from spontaneous reports and electronic health records for detection of adverse drug reactions. *J Am Med Inform Assoc*, 2012 doi:10.1136/amiajnl-2012-000930.
4. Nadkarni PM. Drug safety surveillance using de-identified EMR and claims data: issues and challenges. *J Am Med Inform Assoc*, 2010;**17**:671–674.
5. Tomlin A, Reith D, Dovey S, Tilyard M. Methods for retrospective detection of drug safety signals and adverse events in electronic general practice records. *Drug Saf*, 2012;**35**:733–743.
6. Wilson AM, Thabane L, Holbrook A. Application of data mining techniques in pharmacovigilance. *Br J Clin Pharmacol*, 2004;**57**:127–134.
7. Brown JS, Kulldorff M, Chan KA *et al.* Early detection of adverse drug events within population-based health networks: application of sequential testing methods. *Pharmacoepidemiol Drug Saf*, 2007;**16**:1275–1284.
8. Gagne JJ, Glynn RJ, Rassen JA, Walker AM, Daniel GW, Sridhar G, Schneeweiss S.

Active safety monitoring of newly marketed medications in a distributed data network: application of a semi-automated monitoring system. *Clin Pharmacol Ther*, 2012;**92**:80–86.

9. Tomlin A, Reith D, Dovey S, Tilyard M. Methods for retrospective detection of drug safety signals and adverse events in electronic general practice records. *Drug Saf*, 2012;**35**:733–743.
10. Behrman RE, Benner JS, Brown JS, McClellan M, Woodcock J, Platt R. Developing the sentinel system – a national resource for evidence development. *N Engl J Med*, 2011;**364**:498–499.
11. Platt R, Carnahan RM, Brown JS *et al.* The U.S. Food and Drug Administration's Mini-Sentinel program: status and direction. *Pharmacoepidemiol Drug Saf*, 2012;**21**(Suppl 1):1–8.
12. Avillach P, Coloma PM, Gini R *et al.*; on behalf of the EU-ADR consortium. Harmonization process for the identification of medical events in eight European healthcare databases: the experience from the EU-ADR project. *J Am Med Inform Assoc*, 2013;**20**:184–192.
13. Yoon D, Park MY, Choi NK, Park BJ, Kim JH, Park RW. Detection of adverse drug reaction signals using an electronic health records database: Comparison of the Laboratory Extreme Abnormality Ratio (CLEAR) algorithm. *Clin Pharmacol Ther*, 2012;**91**:467–474.
14. Gau CS, Chang IS, Lin Wu FL *et al.* Usage of the claim database of national health insurance programme for analysis of cisapride-erythromycin co-medication in Taiwan. *Pharmacoepidemiol Drug Saf*, 2007;**16**:86–95.
15. Moghadasian MH, Mancini GB, Frohlich JJ. Pharmacotherapy of hypercholesterolaemia: statins in clinical practice. *Expert Opin Pharmacother*, 2000;**1**:683–695.
16. Ballantyne CM, Corsini A, Davidson MH *et al.* Risk for myopathy with statin therapy in high-risk patients. *Arch Intern Med*, 2003;**163**:553–564.
17. Hamilton-Craig I. Statin-associated myopathy. *Med J Aust*, 2001;**175**:486–489.
18. Shek A, Ferrill MJ. Statin-fibrate combination therapy. *Ann Pharmacother*, 2001;**35**:908–917.
19. Graham DJ, Staffa JA, Shatin D *et al.* Incidence of hospitalized rhabdomyolysis in patients treated with lipid-lowering drugs. *JAMA*, 2004;**292**:2585–2590.
20. Huerta-Alardőn AL, Varon J, Marik PE. Bench-to-bedside review: Rhabdomyolysis - an overview for clinicians. *Crit Care*, 2005;**9**:158–169.
21. Trifirò G, Pariente A, Coloma PM *et al.* Fourrier-Reglat A; EU-ADR group. Data mining on electronic health record databases for signal detection in pharmacovigilance: which events to monitor? *Pharmacoepidemiol Drug Saf*, 2009;**18**:1176–1184.
22. Ramirez E, Carcas AJ, Borobia AM, Lei SH, Piñana E, Fudio S, Frias J. A pharmacovigilance program from laboratory signals for the detection and reporting of serious adverse drug reactions in hospitalized patients. *Clin Pharmacol Ther*, 2010;**87**:74–86.
23. Haerian K, Varn D, Vaidya S, Ena L, Chase HS, Friedman C. Detection of pharmacovigilance-related adverse events using electronic health records and automated methods. *Clin Pharmacol Ther*, 2012;**92**:228–234.
24. Coloma PM, Trifirò G, Schuemie MJ *et al.* Sturkenboom M; EU-ADR Consortium. Electronic healthcare databases for active drug safety surveillance: is there enough leverage? *Pharmacoepidemiol Drug Saf*, 2012;**21**:611–621.
25. Stein HD, Nadkarni P, Erdos J, Miller PL. Exploring the degree of concordance of coded and textual data in answering clinical queries from a clinical data repository. *J Am Med Inform Assoc*, 2000;**7**:42–54.
26. Liu M, McPeek Hinz ER, Matheny ME, Denny JC, Schildcrout JS, Miller RA, Xu H Comparative analysis of pharmacovigilance methods in the detection of adverse drug reactions using electronic medical records. *J Am Med Inform Assoc*, 2012 doi:10.1136/amiajnl-2012-001119. [Epub ahead of print].
27. Park MY, Yoon D, Lee K *et al.* A novel algorithm for detection of adverse drug reaction signals using a hospital electronic medical record database. *Pharmacoepidemiol Drug Saf*, 2011;**20**:598–607.